Light-front dynamics and AdS/QCD correspondence: The pion form factor in the space- and time-like regions

Stanley J. Brodsky[1] and Guy F. de Téramond[1,2]

[1]*Stanford Linear Accelerator Center, Stanford University, Stanford, California 94309, USA*
[2]*Universidad de Costa Rica, San José, Costa Rica*

(Received 13 October 2007; published 17 March 2008)

The AdS/CFT correspondence between string theory in AdS space and conformal field theories in physical space-time leads to an analytic, semiclassical model for strongly-coupled QCD which has scale invariance and dimensional counting at short distances and color confinement at large distances. The AdS/CFT correspondence also provides insights into the inherently nonperturbative aspects of QCD such as the orbital and radial spectra of hadrons and the form of hadronic wavefunctions. In particular, we show that there is an exact correspondence between the fifth-dimensional coordinate of anti–de Sitter (AdS) space z and a specific light-front impact variable ζ which measures the separation of the quark and gluonic constituents within the hadron in ordinary space-time. This connection allows one to compute the analytic form of the frame-independent light-front wavefunctions of mesons and baryons, the fundamental entities which encode hadron properties and which allow the computation of decay constants, form factors and other exclusive scattering amplitudes. Relativistic light-front equations in ordinary space-time are found which reproduce the results obtained using the fifth-dimensional theory. As specific examples we compute the pion coupling constant f_π, the pion charge radius $\langle r_\pi^2 \rangle$ and examine the propagation of the electromagnetic current in AdS space, which determines the space and timelike behavior of the pion form factor and the pole of the ρ meson.

DOI: 10.1103/PhysRevD.77.056007 PACS numbers: 11.15.Tk, 11.25.Tq, 12.38.Aw, 12.40.Yx

I. INTRODUCTION

Quantum chromodynamics, the Yang-Mills local gauge field theory of $SU(3)_C$ color symmetry provides a fundamental description of hadron and nuclear physics in terms of quark and gluon degrees of freedom. However, because of its strong coupling nature, it is difficult to find analytic solutions to QCD or to make precise predictions outside of its perturbative domain. An important goal is thus to find an initial approximation to QCD which is both analytically tractable and which can be systematically improved. For example, in quantum electrodynamics, the Coulombic Schrödinger and Dirac equations provide quite accurate first approximations to atomic bound state problems, which can then be systematically improved using the Bethe-Salpeter formalism and correcting for quantum fluctuations, such as the Lamb shift and vacuum polarization.

One of the most significant theoretical advances in recent years has been the application of the AdS/CFT correspondence [1] between string states defined on the 5-dimensional anti–de Sitter (AdS) space-time and conformal field theories in physical space-time. The essential principle underlying the AdS/CFT approach to conformal gauge theories is the isomorphism of the group of Poincaré and conformal transformations $SO(4, 2)$ to the group of isometries of anti–de Sitter space. The AdS metric is

$$ds^2 = \frac{R^2}{z^2}(\eta_{\mu\nu} dx^\mu dx^\nu - dz^2), \tag{1}$$

which is invariant under scale changes of the coordinate in the fifth dimension $z \to \lambda z$ and $x_\mu \to \lambda x_\mu$. Thus one can match scale transformations of the theory in $3 + 1$ physical space-time to scale transformations in the fifth dimension z.

QCD is not itself a conformal theory; however as we shall discuss, there are indications, both from theory and phenomenology, that the QCD coupling is slowly varying at small momentum transfer. Thus in the domain where the QCD coupling is approximately constant and quark masses can be neglected, QCD resembles a conformal theory. As shown by Polchinski and Strassler [2], one can simulate confinement by imposing boundary conditions in the holographic variable at $z = z_0 = 1/\Lambda_{\rm QCD}$. Confinement can also be introduced by modifying the AdS metric to mimic a confining potential. The resulting models, although *ad hoc*, provide a simple semiclassical approximation to QCD which has both constituent counting rule behavior at short distances and confinement at large distances. This simple approach, which has been described as a ''bottom-up'' approach, has been successful in obtaining general properties of scattering amplitudes of hadronic bound states at strong coupling [2–5], the low-lying hadron spectra [6–15], hadron couplings and chiral symmetry breaking [9,16–18], quark potentials in confining backgrounds [19,20] and a description of weak hadron decays [21]. Geometry backreaction in AdS may also be relevant to the infrared physics [22]. The gauge theory/gravity duality also provides a convenient framework for the description of deep inelastic scattering structure functions at small x [23], a unified description of hard and soft pomeron physics [24] and gluon scattering amplitudes at strong coupling [25]. Recent applications to describe chiral symmetry

breaking [26] and other meson and baryon properties have also been carried out within the framework of a top-bottom approach to AdS/CFT using higher dimensional branes [27–31].

The AdS/QCD correspondence is particularly relevant for the description of hadronic form factors, since it incorporates the connection between the twist of the hadron to the falloff of its current matrix elements, as well as essential aspects of vector meson dominance. It also provides a convenient framework for analytically continuing the spacelike results to the timelike region. Recent applications to the form factors of mesons and nucleons [11,32–37] have followed from the original work described in [23,38]

A physical hadron in four-dimensional Minkowski space has four-momentum P_μ and invariant mass given by $P_\mu P^\mu = \mathcal{M}^2$. The physical states in AdS_5 space are represented by normalizable ''string'' modes

$$\Phi_P(x, z) \sim e^{-iP\cdot x}\Phi(z), \tag{2}$$

with plane waves along the Poincaré coordinates and a profile function $\Phi(z)$ along the holographic coordinate z. For small z, Φ scales as $\Phi \sim z^\Delta$, where Δ is the conformal dimension of the string state, the same dimension of the interpolating operator $\mathcal{O}$ which creates a hadron out of the vacuum [2], $\langle P|\mathcal{O}|0\rangle \neq 0$. The scale dependence of each string mode $\Phi(x, z)$ is thus determined by matching its behavior at $z \to 0$ with the dimension of the corresponding hadronic state at short distances $x^2 \to 0$. Changes in length scale are mapped to evolution in the holographic variable z. The string mode in z thus represents the extension of the hadron wave function into the fifth dimension. There are also non-normalizable modes which are related to external currents: they propagate into the interior of AdS space.

As we shall discuss, there is a remarkable mapping between the AdS description of hadrons and the Hamiltonian formulation of QCD in physical space-time quantized on the light front. The light-front wavefunctions of bound states in QCD are relativistic and frame-independent generalizations of the familiar Schrödinger wavefunctions of atomic physics, but they are determined at fixed light-cone time $\tau = t + z/c$—the ''front form'' advocated by Dirac—rather than at fixed ordinary time t. An important feature of light-front quantization is the fact that it provides exact formulas to write down matrix elements as a sum of bilinear forms, which can be mapped into their AdS/CFT counterparts in the semiclassical approximation. One can thus obtain not only an accurate description of the hadron spectrum for light quarks, but also a remarkably simple but realistic model of the valence wavefunctions of mesons, baryons, and glueballs. In fact, we find an exact correspondence between the fifth-dimensional coordinate of anti–de Sitter space z and a specific impact variable ζ in the light-front formalism which measures the separation of the constituents within the hadron in ordinary space-time. Since $\tau = 0$ in the front form, it corresponds to the transverse separation $x^\mu x_\mu = -\mathbf{x}_\perp^2$. The amplitude $\Phi(z)$ describing the hadronic state in AdS_5 can then be precisely mapped to the light-front wavefunctions $\psi_{n/h}$ of hadrons in physical space-time [39], thus providing a relativistic description of hadrons in QCD at the amplitude level.

This paper is organized as follows. We first review in Sec. II recent evidence which indicates that QCD has near-conformal behavior in the infrared region. The QCD light-front Fock representation is then briefly reviewed in Sec. III. In Sec. IV, we derive the exact form of current matrix elements in the light-front formalism which sets the framework for the identification with the corresponding amplitudes in AdS/CFT, and constitutes the basis of the partonic interpretation of the AdS/CFT correspondence. The actual mapping to AdS matrix elements is carried out in Sec. V for the hard-wall model and in Sec. VI for the soft-wall model, where the truncated space boundary conditions are replaced by a smooth cutoff. Results for the pion form factor in the space and timelike regions and the pion charge radius $\langle r_\pi^2\rangle$ are presented in Sec. VII for both models. In Sec. VIII we compute the pion decay constant in light-front QCD and find its precise expression in AdS, following the mapping discussed in Secs. V and VI. Some final remarks are given in the conclusions in Sec. IX. Other technical aspects useful for the discussion of the article are given in the appendices. In particular we relate our results for the soft-wall model to the analytical results found recently by Grigoryan and Radyushkin [36].

II. CONFORMAL QCD WINDOW

It was originally believed that the AdS/CFT mathematical correspondence could only be applied to strictly conformal theories, such as $\mathcal{N} = 4$ supersymmetric Yang-Mills gauge theory. In our approach, we will apply the gauge theory/gravity duality to the strong coupling regime of QCD where the coupling appears to be approximately constant. Theoretical studies based on the Dyson-Schwinger equation [40–43] and phenomenological [44,45] evidence are in fact accumulating that the QCD couplings defined from physical observables such as τ decay [46] become constant at small virtuality; i.e., effective charges develop an infrared fixed point in contradiction to the usual assumption of singular growth in the infrared. Recent lattice gauge theory simulations [47] also indicate an infrared fixed point for QCD. The near-constant behavior of effective couplings thus suggests that QCD can be approximated as a conformal theory at relatively small momentum transfer.

It is clear from a physical perspective that in a confining theory where gluons and quarks have an effective mass or maximal wavelength, all vacuum polarization corrections to the gluon self-energy must decouple at long wavelength; thus an infrared fixed point appears to be a natural con-

sequence of confinement. Furthermore, if one considers a semiclassical approximation to QCD with massless quarks and without particle creation or absorption, then the resulting β function is zero, the coupling is constant, and the approximate theory is scale and conformal invariant.

In the case of hard exclusive reactions [48], the virtuality of the gluons exchanged in the underlying QCD process is typically much less than the momentum transfer scale Q, since typically several gluons share the total momentum transfer. Since the coupling is probed in the conformal window, this kinematic feature can explain why the measured proton Dirac form factor scales as $Q^4 F_1(Q^2) \simeq$ const up to $Q^2 < 35$ GeV^2 [49] with little sign of the logarithmic running of the QCD coupling.

Thus conformal symmetry can be a useful first approximant even for physical QCD. Conformal symmetry is broken in physical QCD by quantum effects and quark masses; nevertheless, one can use conformal symmetry as a *template*, systematically correcting for its nonzero β function as well as higher-twist effects. For example, "commensurate scale relations" [50] which relate QCD observables to each other, such as the generalized Crewther relation [51], have no renormalization scale or scheme ambiguity and retain a convergent perturbative structure which reflects the underlying conformal symmetry of the classical theory. In general, the scale is set such that one has the correct analytic behavior at the heavy particle thresholds [52]. Analytic effective charges [53] such as the pinch scheme [54,55] also provide an important perspective for unifying the electroweak and strong couplings [56].

III. THE LIGHT-FRONT FOCK REPRESENTATION

The light-front expansion of any hadronic system is constructed by quantizing quantum chromodynamics at fixed light-front time [57] $\tau = t + z/c$. In terms of the hadron four-momentum $P = (P^+, P^-, \mathbf{P}_\perp)$, $P^\pm = P^0 \pm P^3$, the light-front Lorentz-invariant Hamiltonian for the composite system, $H_{\rm LF}^{\rm QCD} = P^- P^+ - \mathbf{P}_\perp^2$, has eigenvalues given in terms of the eigenmass $\mathcal{M}$ squared corresponding to the mass spectrum of the color-singlet states in QCD [58]. The momentum generators P^+ and $\mathbf{P}_\perp$ are kinematical; i.e., they are independent of the interactions. The LF time evolution operator $P^- = i\frac{d}{d\tau}$ can be derived directly from the QCD Lagrangian in the light-front gauge $A^+ = 0$. In principle, the complete set of bound state and scattering eigensolutions of $H_{\rm LF}$ can be obtained by solving the light-front Heisenberg equation

$$H_{\rm LF}|\psi_h\rangle = \mathcal{M}_h^2|\psi_h\rangle, \tag{3}$$

where $|\psi_h\rangle$ is an expansion in multiparticle Fock eigenstates $\{|n\rangle\}$ of the free light-front (LF) Hamiltonian: $|\psi_h\rangle = \sum_n \psi_{n/h}|\psi_h\rangle$. The LF Heisenberg equation has in fact been solved for QCD(1 + 1) and a number of other theories using the discretized light-cone quantization method [59]. The light-front gauge has the advantage that all gluon degrees of freedom have physical polarization and positive metric. In addition, orbital angular momentum has a simple physical interpretation in this representation. The light-front wavefunctions (LFWFs) $\psi_{n/h}$ provide a frame-independent representation of a hadron, and relate the quark and gluon degrees of freedom with their asymptotic hadronic state.

Given the light-front wavefunctions $\psi_{n/h}$ one can compute a large range of hadron observables. For example, the valence and sea quark and gluon distributions which are measured in deep inelastic lepton scattering are defined from the squares of the LFWFs summed over all Fock states n. Form factors, exclusive weak transition amplitudes [60] such as $B \to \ell\nu\pi$, and the generalized parton distributions [61] measured in deeply virtual Compton scattering are (assuming the "handbag" approximation) overlaps of the initial and final LFWFs with $n = n'$ and $n = n' + 2$. The gauge-invariant distribution amplitude $\phi_H(x_i, Q)$ defined from the integral over the transverse momenta $\mathbf{k}_{\perp i}^2 \le Q^2$ of the valence (smallest n) Fock state provides a fundamental measure of the hadron at the amplitude level [62,63]; they are the nonperturbative input to the factorized form of hard exclusive amplitudes and exclusive heavy hadron decays in perturbative QCD. The resulting distributions obey the Dokshitzer-Gribov-Lipatov-Altarelli-Parisi (DGLAP) and Efremov-Radyushkin-Brodsky-Lepage evolution equations as a function of the maximal invariant mass, thus providing a physical factorization scheme [48]. In each case, the derived quantities satisfy the appropriate operator product expansions, sum rules and evolution equations. At large x where the struck quark is far-off shell, DGLAP evolution is quenched [64], so that the falloff of the deep inelastic scattering cross sections in Q^2 satisfies inclusive-exclusive duality at fixed W^2.

The hadron wavefunction is an eigenstate of the total momentum P^+ and $\mathbf{P}_\perp$ and the longitudinal spin projection S_z, and is normalized according to

$$\langle\psi_h(P^+, \mathbf{P}_\perp, S_z)|\psi_h(P'^+, \mathbf{P}'_\perp, S'_z)\rangle = 2P^+(2\pi)^3\delta_{S_z,S'_z}\delta(P^+ - P'^+)\delta^{(2)}(\mathbf{P}_\perp - \mathbf{P}'_\perp). \tag{4}$$

Each hadronic eigenstate $|\psi_h\rangle$ is expanded in a Fock-state complete basis of noninteracting n-particle states $|n\rangle$ with an infinite number of components

$$|\psi_h(P^+, \mathbf{P}_\perp, S_z)\rangle = \sum_{n,\lambda i}\prod_{i=1}^{n}\int \frac{dx_i d^2\mathbf{k}_{\perp i}}{2\sqrt{x_i}(2\pi)^3}(16\pi^3)\delta\Big(1 - \sum_{j=1}^{n} x_j\Big)\delta^{(2)}\Big(\sum_{j=1}^{n}\mathbf{k}_{\perp j}\Big) \times \psi_{n/h}(x_i, \mathbf{k}_{\perp i}, \lambda_i)|n\colon x_i P^+, x_i\mathbf{P}_\perp + \mathbf{k}_{\perp i}, \lambda_i\rangle, \tag{5}$$

where the sum begins with the valence state; e.g., $n \ge 2$ for mesons. The coefficients of the Fock expansion

$$\psi_{n/h}(x_i, \mathbf{k}_{\perp i}, \lambda_i) = \langle n\colon x_i, \mathbf{k}_{\perp i}, \lambda_i | \psi_h \rangle, \tag{6}$$

are independent of the total momentum P^+ and $\mathbf{P}_\perp$ of the hadron and depend only on the relative partonic coordinates, the longitudinal momentum fraction $x_i = k_i^+/P^+$, the relative transverse momentum $\mathbf{k}_{\perp i}$, and λ_i, the projection of the constituent's spin along the z direction. Thus, given the Fock-projection (6), the wavefunction of a hadron is determined in any frame. The amplitudes $\psi_{n/h}$ represent the probability amplitudes to find on-mass-shell constituents i with longitudinal momentum $x_i P^+$, transverse momentum $x_i \mathbf{P}_\perp + \mathbf{k}_{\perp i}$, helicity λ_i and invariant mass

$$\mathcal{M}_n^2 = \sum_{i=1}^n k_i^\mu k_{i\mu} = \sum_{i=1}^n \frac{\mathbf{k}_{\perp i}^2 + m_i^2}{x_i}, \tag{7}$$

in the hadron h. Momentum conservation requires $\sum_{i=1}^n x_i = 1$ and $\sum_{i=1}^n \mathbf{k}_{\perp i} = 0$. In addition, each light-front wavefunction $\psi_{n/h}(x_i, \mathbf{k}_{\perp i}, \lambda_i)$ obeys the angular momentum sum rule [65]

$$J^z = \sum_{i=1}^n S_i^z + \sum_{i=1}^{n-1} L_i^z, \tag{8}$$

where $S_i^z = \lambda_i$ and the $n-1$ orbital angular momenta have the operator form

$$L_i^z = -i\left(\frac{\partial}{\partial k_i^x} k_i^y - \frac{\partial}{\partial k_i^y} k_i^x\right). \tag{9}$$

The LFWFs are normalized according to

$$\sum_n \int [dx_i][d^2\mathbf{k}_{\perp i}] |\psi_{n/h}(x_i, \mathbf{k}_{\perp i})|^2 = 1, \tag{10}$$

where the measure of the constituents phase-space momentum integration is

$$\int [dx_i] \equiv \prod_{i=1}^n \int dx_i \, \delta\left(1 - \sum_{j=1}^n x_j\right), \tag{11}$$

$$\int [d^2\mathbf{k}_{\perp i}] \equiv \prod_{i=1}^n \int \frac{d^2\mathbf{k}_{\perp i}}{2(2\pi)^3} (16\pi^3) \delta^{(2)}\left(\sum_{j=1}^n \mathbf{k}_{\perp j}\right), \tag{12}$$

for the normalization given by (4). The spin indices have been suppressed.

A. Construction of partonic states

The complete basis of Fock states $|n\rangle$ is constructed by applying free-field creation operators to the vacuum state $|0\rangle$ which has no particle content, $P^+|0\rangle = 0$, $\mathbf{P}_\perp|0\rangle = 0$. The basic constituents appear from the light-front quantization of the excitations of the dynamical fields, the Dirac field ψ_+, $\psi_\pm = \Lambda_\pm \psi$, $\Lambda_\pm = \gamma^0\gamma^\pm$, and the transverse field $\mathbf{A}_\perp$ in the $A^+ = 0$ gauge, expanded in terms of creation and annihilation operators on the transverse plane with coordinates $x^- = x^0 - x^3$ and $\mathbf{x}_\perp$ at fixed light-front time $x^+ = x^0 + x^3$ [58];

$$\psi_+(x)_\alpha = \sum_\lambda \int_{q^+>0} \frac{dq^+}{\sqrt{2q^+}} \frac{d^2\mathbf{q}_\perp}{(2\pi)^3} \times [b_\lambda(q) u_\alpha(q, \lambda) e^{-iq\cdot x} + d_\lambda(q)^\dagger v_\alpha(q, \lambda) e^{iq\cdot x}], \tag{13}$$

$$\mathbf{A}_\perp(x) = \sum_\lambda \int_{q^+>0} \frac{dq^+}{\sqrt{2q^+}} \frac{d^2\mathbf{q}_\perp}{(2\pi)^3} \times [a(q) \vec{\epsilon}_\perp(q, \lambda) e^{-iq\cdot x} + a(q)^\dagger \vec{\epsilon}_\perp^*(q, \lambda) e^{iq\cdot x}], \tag{14}$$

with commutation relations

$$[a(q), a^\dagger(q')] = \{b(q), b^\dagger(q')\} = \{d(q), d^\dagger(q')\} = (2\pi)^3 \delta(q^+ - q'^+) \delta^{(2)}(\mathbf{q}_\perp - \mathbf{q}'_\perp). \tag{15}$$

We shall use the conventions of Appendix A of Ref. [48] for the properties of the light-cone spinors. A one-particle state is defined by

$$|q\rangle = \sqrt{2q^+} b^\dagger(q)|0\rangle, \tag{16}$$

so that its normalization has the Lorentz-invariant form

$$\langle q|q'\rangle = 2q^+(2\pi)^3 \delta(q^+ - q'^+) \delta^{(2)}(\mathbf{q}_\perp - \mathbf{q}'_\perp), \tag{17}$$

and this fixes our normalization. Each n-particle Fock state $|p_i^+, \mathbf{p}_{\perp i}\rangle$ is an eigenstate of P^+ and $\mathbf{P}_\perp$ and is normalized according to

$$\langle p_i^+, \mathbf{p}_{\perp i}, \lambda | p_i'^+, \mathbf{p}'_{\perp i}, \lambda' \rangle = 2p_i^+(2\pi)^3 \delta(p_i^+ - p_i'^+) \times \delta^{(2)}(\mathbf{p}_{\perp i} - \mathbf{p}'_{\perp i}) \delta_{\lambda,\lambda'}. \tag{18}$$

B. Impact space representation

The holographic mapping of hadronic LFWFs to AdS string modes is most transparent when one uses the impact parameter space representation. The total position coordinate of a hadron or its transverse center of momentum $\mathbf{R}_\perp$ is defined in terms of the energy momentum tensor $T^{\mu\nu}$

$$\mathbf{R}_\perp = \frac{1}{P^+} \int dx^- \int d^2\mathbf{x}_\perp T^{++} \mathbf{x}_\perp. \tag{19}$$

In terms of partonic transverse coordinates

$$x_i \mathbf{r}_{\perp i} = x_i \mathbf{R}_\perp + \mathbf{b}_{\perp i}, \tag{20}$$

where the $\mathbf{r}_{\perp i}$ are the physical transverse position coordinates and the $\mathbf{b}_{\perp i}$ frame-independent internal coordinates, conjugate to the relative coordinates $\mathbf{k}_{\perp i}$. Thus, $\sum_{i=1}^n \mathbf{b}_{\perp i} = 0$ and $\mathbf{R}_\perp = \sum_{i=1}^n x_i \mathbf{r}_{\perp i}$. The LFWFs $\psi_n(x_j, \mathbf{k}_{\perp j})$ can be expanded in terms of the $n-1$ independent transverse coordinates $\mathbf{b}_{\perp j}$, $j = 1, 2, \ldots, n-1$

$$\psi_n(x_j, \mathbf{k}_{\perp j}) = (4\pi)^{(n-1)/2} \prod_{j=1}^{n-1} \int d^2\mathbf{b}_{\perp j} \times \exp\Big(i \sum_{j=1}^{n-1} \mathbf{b}_{\perp j} \cdot \mathbf{k}_{\perp j}\Big) \tilde{\psi}_n(x_j, \mathbf{b}_{\perp j}). \quad (21)$$

The normalization is defined by

$$\sum_n \prod_{j=1}^{n-1} \int dx_j d^2\mathbf{b}_{\perp j} |\tilde{\psi}_n(x_j, \mathbf{b}_{\perp j})|^2 = 1. \quad (22)$$

IV. THE FORM FACTOR IN QCD

The hadron form factors can be predicted from the overlap integral of string modes propagating in AdS space with the boundary electromagnetic source which probes the AdS interior, or equivalently by using the Drell-Yan-West formula in physical space-time. If both quantities represent the same physical observable for any value of the transfer momentum q^2, an exact correspondence can be established between the string modes Φ in fifth-dimensional AdS space and the light-front wavefunctions of hadrons $\psi_{n/h}$ in 3 + 1 space-time [39].

A. The Drell-Yan-West form factor

The light-front formalism provides an exact Lorentz-invariant representation of current matrix elements in terms of the overlap of light-front wave functions. The electromagnetic current has elementary couplings to the charged constituents since the full Heisenberg current can be replaced by the free quark current $J^\mu(0)$, evaluated at fixed light-cone time $x^+ = 0$ in the $q^+ = 0$ frame [66]. In contrast to the covariant Bethe-Salpeter equation, in the light-front Fock expansion one does not need to include the contributions to the current from an infinite number of irreducible kernels, or the interactions of the electromagnetic current with vacuum fluctuations [58].

We choose the light-front frame coordinates

$$P = (P^+, P^-, \mathbf{P}_\perp) = \Big(P^+, \frac{M^2}{P^+}, \vec{0}_\perp\Big),$$
$$q = (q^+, q^-, \mathbf{q}_\perp) = \Big(0, \frac{2q \cdot P}{P^+}, \mathbf{q}_\perp\Big), \quad (23)$$

where $q^2 = -Q^2 = -2q \cdot P = -\mathbf{q}_\perp^2$ is the spacelike four-momentum squared transferred to the composite system. The electromagnetic form factor of a meson is defined in terms of the hadronic amplitude of the electromagnetic current evaluated at light-cone time $x^+ = 0$

$$\langle P'|J^+(0)|P\rangle = 2(P + P')^+ F(Q^2), \quad (24)$$

where $P' = P + q$ and $F(0) = 1$.

The expression for the current operator $J^+(x) = \sum_q e_q \bar{\psi}(x)\gamma^+\psi(x)$ in the particle number representation follows from the momentum expansion of $\psi(x)$ in terms of creation and annihilation operators given by (13). Since γ^+ conserves the spin component of the struck quark (Appendix A), we obtain for $J^+(0)$

$$J + (0) = \sum_q e_q \int \frac{dq^+ d^2\mathbf{q}_\perp}{(2\pi)^3} \int \frac{dq'^+ d^2\mathbf{q}'_\perp}{(2\pi)^3} \{b_\uparrow^\dagger(q) b_\uparrow(q') + b_\downarrow^\dagger(q) b_\downarrow(q') - d_\uparrow^\dagger(q) d_\uparrow(q') - d_\downarrow^\dagger(q) d_\downarrow(q')\}. \quad (25)$$

The operator J annihilates a quark (antiquark) with charge e_q ($-e_q$), momentum q' and spin-up (spin-down) along the z direction and creates a quark (antiquark) with the same spin and momentum q.

The matrix element $\langle\psi_{P'}|J^+(0)|\psi_P\rangle$ can be computed by expanding the initial and final hadronic states in terms of its Fock components using (5). The transition amplitude can then be expressed as a sum of overlap integrals with diagonal J^+-matrix elements in the n-particle Fock-state basis. For each Fock-state, we label with q the struck constituent quark with charge e_q and $j = 1, 2 \ldots, n-1$ each spectator. Using the normalization condition (18) for each individual constituent and after integration over the intermediate variables in the $q^+ = 0$ frame, we find the Drell-Yan-West (DYW) expression for the meson form factor [66,67]

$$F(q^2) = \sum_n \int [dx_i] \times [d^2\mathbf{k}_{\perp i}] \sum_j e_j \psi^*_{n/P'}(x_i, \mathbf{k}'_{\perp i}, \lambda_i) \psi_{n/P}(x_i, \mathbf{k}_{\perp i}, \lambda_i), \quad (26)$$

where the variables of the light-cone Fock components in the final state are given by $\mathbf{k}'_{\perp i} = \mathbf{k}_{\perp i} + (1 - x_i)\mathbf{q}_\perp$ for a struck constituent quark and $\mathbf{k}'_{\perp i} = \mathbf{k}_{\perp i} - x_i\mathbf{q}_\perp$ for each spectator. The formula is exact if the sum is over all Fock states n. Notice that there is a factor of N_C from a closed quark loop where the photon is attached and a normalization factor of $1/\sqrt{N_C}$ for each meson wave function; thus color factors cancel out from the expression of the form factor.

B. The form factor in impact space

One of the important advantages of the light-front formalism is that current matrix elements can be represented without approximation as overlaps of light-front wavefunctions. In the case of the elastic spacelike form factors, the matrix element of the J^+ current only couples Fock states with the same number of constituents, as expressed by the Drell-Yan-West formula (26). Suppose that the charged parton n is the active constituent struck by the current, and the quarks $i = 1, 2, \cdots, n-1$ are spectators. We substitute (21) in the DYW formula (26). Integration over $k_\perp$ phase space gives us $n - 1$ delta functions to integrate over the $n - 1$ intermediate transverse variables

with the result

$$F(q^2) = \sum_n \prod_{j=1}^{n-1} \int dx_j d^2\mathbf{b}_{\perp j} \exp\Big(i\mathbf{q}_\perp \cdot \sum_{j=1}^{n-1} x_j \mathbf{b}_{\perp j}\Big) \times |\tilde{\psi}_n(x_j, \mathbf{b}_{\perp j})|^2, \quad (27)$$

corresponding to a change of transverse momentum $x_j\mathbf{q}_\perp$ for each of the $n-1$ spectators. This is a convenient form for comparison with AdS results, since the form factor may be expressed in terms of the product of light-front wave functions with identical variables.

C. Effective single-particle distribution

The form factor in the light-front formulation has an exact representation in terms of an effective single-particle density [68]

$$F(q^2) = \int_0^1 dx \rho(x, \mathbf{q}_\perp), \quad (28)$$

where $\rho(x, \mathbf{q}_\perp)$ is given by

$$\rho(x, \mathbf{q}_\perp) = \sum_n \prod_{j=1}^{n-1} \int dx_j d^2\mathbf{b}_{\perp j} \delta\Big(1 - x - \sum_{j=1}^{n-1} x_j\Big) \times \exp\Big(i\mathbf{q}_\perp \cdot \sum_{j=1}^{n-1} x_j \mathbf{b}_{\perp j}\Big) |\tilde{\psi}_n(x_j, \mathbf{b}_{\perp j})|^2. \quad (29)$$

The integration is over the coordinates of the $n-1$ spectator partons, and $x = x_n$ is the coordinate of the active charged quark. We can also write the form factor in terms of an effective single-particle transverse distribution $\tilde{\rho}(x, \vec{\eta}_\perp)$ [68]

$$F(q^2) = \int_0^1 dx \int d^2\vec{\eta}_\perp e^{i\vec{\eta}_\perp \cdot \mathbf{q}_\perp} \tilde{\rho}(x, \vec{\eta}_\perp), \quad (30)$$

where $\vec{\eta}_\perp = \sum_{j=1}^{n-1} x_j \mathbf{b}_{\perp j}$ is the x-weighted transverse position coordinate of the $n-1$ spectators [69]. The corresponding transverse density is

$$\tilde{\rho}(x, \vec{\eta}_\perp) = \int \frac{d^2\mathbf{q}_\perp}{(2\pi)^2} e^{-i\vec{\eta}_\perp \cdot \mathbf{q}_\perp} \rho(x, \mathbf{q}_\perp) = \sum_n \prod_{j=1}^{n-1} \int dx_j d^2\mathbf{b}_{\perp j} \delta\Big(1 - x - \sum_{j=1}^{n-1} x_j\Big) \times \delta^{(2)}\Big(\sum_{j=1}^{n-1} x_j \mathbf{b}_{\perp j} - \vec{\eta}_\perp\Big) |\tilde{\psi}_n(x_j, \mathbf{b}_{\perp j})|^2. \quad (31)$$

The procedure is valid for any Fock state n, and thus the results can be summed over n to obtain an exact representation.

V. THE FORM FACTOR IN ADS/CFT AND LIGHT-FRONT MAPPING OF STRING AMPLITUDES

We now derive the corresponding expression for the electromagnetic form factor of a pion in AdS. The derivation can be extended to vector mesons and baryons, although the actual analysis becomes more complex, since the matrix elements of spacelike local operators include the dependence for the different spin transitions. For example, in the case of the proton, the Dirac and Pauli form factors correspond to the light-cone spin-conserving and spin-flip matrix elements of the J^+ current [70], and a mapping to the corresponding AdS matrix elements has to be carried out for each case. The electric vector-meson form factor has been discussed recently in the context of the hard-wall model in [35,38] and in the soft-wall model in [36]. A detailed discussion of the form factor of nucleons in AdS/QCD will be given elsewhere.

In AdS/CFT, the hadronic matrix element for the electromagnetic current has the form of a convolution of the string modes for the initial and final hadrons with the external electromagnetic source which propagates inside AdS. We discuss first the truncated space or hard wall [2] holographic model, where quarks and gluons as well as the external electromagnetic current propagate freely into the AdS interior according to the AdS metric. We discuss later the case where the sharp boundary of the hard wall in the infrared region is replaced by the introduction of a soft cutoff.

AdS coordinates are the Minkowski coordinates x^μ and z, the holographic coordinate, which we label collectively $x^\ell = (x^\mu, z)$. The metric of the full space-time is

$$ds^2 = g_{\ell m} dx^\ell dx^m \quad (32)$$

where $g_{\ell m} \to (R^2/z^2)\eta_{\ell m}$ in the conformal $z \to 0$ limit, and $\eta_{\ell m}$ has diagonal components $(1, -1, \cdots, -1)$. Unless stated otherwise, 5-dimensional fields are represented by capital letters such as Φ. Holographic fields in 4-dimensional Minkowski space are represented by lower case letters such as ϕ. The metric (32) is AdS in the finite interval $0 \le z \le z_0 = 1/\Lambda_{\mathrm{QCD}}$, and the dual conformal field theory is strongly coupled at all scales up to the confining scale.

Assuming minimal coupling the form factor has the form [23,38]

$$ig_5 \int d^4x dz \sqrt{g} A^\ell(x, z) \Phi^*_{P'}(x, z) \overleftrightarrow{\partial}_\ell \Phi_P(x, z), \quad (33)$$

where g_5 is a five-dimensional effective coupling constant and $\Phi_P(x, z)$ is a normalizable mode representing a hadronic state, $\Phi_P(x, z) \sim e^{-iP\cdot x}\Phi(z)$, with hadronic invariant mass given by $P_\mu P^\mu = \mathcal{M}^2$.

We consider the propagation inside AdS space of an electromagnetic probe polarized along Minkowski coordinates ($Q^2 = -q^2 > 0$)

$$A(x,z)_\mu = \epsilon_\mu e^{-iQ\cdot x} J(Q^2,z), \qquad A_z = 0, \tag{34}$$

where $J(Q^2,z)$ has the value 1 at zero momentum transfer, since we are normalizing the bulk solutions to the total charge operator, and as boundary limit the external current $A_\mu(x, z \to 0) = \epsilon_\mu e^{-iQ\cdot x}$. Thus

$$J(Q^2 = 0, z) = J(Q^2, z = 0) = 1. \tag{35}$$

The propagation of the external current inside AdS space is described by the AdS wave equation

$$[z^2\partial_z^2 - z\partial_z - z^2Q^2]J(Q^2,z) = 0, \tag{36}$$

and its solution subject to the boundary conditions (35) is

$$J(Q^2,z) = zQK_1(zQ). \tag{37}$$

Notice that $J(Q^2,z)$ can also be obtained from the Green's function of (36), since it is the bulk-to-boundary propagator [9,38].

Substituting the normalizable mode $\Phi(x,z)$ in (33) and extracting an overall delta function from momentum conservation at the vertex, we find for the elastic form factor of the pion

$$\langle P'|J^\mu(0)|P\rangle = 2(P+P')^\mu F(Q^2), \tag{38}$$

with

$$F(Q^2) = R^3 \int \frac{dz}{z^3}\Phi(z)J(Q^2,z)\Phi(z). \tag{39}$$

The form factor in AdS is thus represented as the overlap in the fifth dimension coordinate z of the normalizable modes dual to the incoming and outgoing hadrons, Φ_P and $\Phi_{P'}$, with the non-normalizable mode, $J(Q^2,z)$, dual to the external source [23]. Since $K_n(x) \sim \sqrt{\pi/2x}e^{-x}$ for large x, it follows that the external electromagnetic field is suppressed inside the AdS cavity for large Q. At small z the string modes scale as $\Phi \sim z^\Delta$. At large enough Q, the important contribution to (39) is from the region near $z \sim 1/Q$

$$F(Q^2) \to \left[\frac{1}{Q^2}\right]^{\Delta-1}, \tag{40}$$

and the ultraviolet pointlike behavior [71] responsible for the power law scaling [72,73] is recovered. This is a remarkable consequence of truncating AdS space [2], since we are indeed describing the coupling of an electromagnetic current to an extended mode, and we should expect soft collision amplitudes characteristic of strings, instead of hard pointlike ultraviolet behavior [2].

A. Light-front mapping in the hard-wall model

We can now establish a connection of the AdS/CFT and the LF formulas. It is useful to integrate (30) over angles to obtain

$$F(q^2) = 2\pi \int_0^1 dx \frac{(1-x)}{x} \int \zeta d\zeta J_0\left(\zeta q\sqrt{\frac{1-x}{x}}\right)\tilde{\rho}(x,\zeta), \tag{41}$$

where we have introduced the variable

$$\zeta = \sqrt{\frac{x}{1-x}}\left|\sum_{j=1}^{n-1} x_j \mathbf{b}_{\perp j}\right|, \tag{42}$$

representing the x-weighted transverse impact coordinate of the spectator system. We substitute the integral representation of the bulk-to boundary propagator $J(Q^2,z)$ (Appendix B)

$$J(Q^2,z) = \int_0^1 dx J_0\left(\zeta Q\sqrt{\frac{1-x}{x}}\right) = \zeta QK_1(\zeta Q), \tag{43}$$

in the expression for the form factor in AdS space (39) for arbitrary values of Q. Comparing with the light-front expression (41), we can identify the spectator density function appearing in the light-front formalism with the corresponding AdS density

$$\tilde{\rho}(x,\zeta) = \frac{R^3}{2\pi}\frac{x}{1-x}\frac{|\Phi(\zeta)|^2}{\zeta^4}. \tag{44}$$

Equation (44) gives a precise relation between string modes $\Phi(\zeta)$ in AdS_5 and the QCD transverse charge density $\tilde{\rho}(x,\zeta)$. The variable ζ, $0 \le \zeta \le \Lambda_{\rm QCD}^{-1}$, represents a measure of the transverse separation between pointlike constituents, and it is also the holographic variable z [39].

In the case of a two-parton constituent bound state the correspondence between the string amplitude $\Phi(z)$ in AdS space and the QCD light-front wave wavefunction $\tilde{\psi}(x,\mathbf{b}_\perp)$ follows immediately from (44). For two partons the transverse density (31) has the simple form

$$\tilde{\rho}_{\,n=2}(x,\zeta) = \frac{|\tilde{\psi}(x,\zeta)|^2}{(1-x)^2}, \tag{45}$$

and a closed form solution for the two-constituent bound state light-front wave function is obtained,

$$|\tilde{\psi}(x,\zeta)|^2 = \frac{R^3}{2\pi}x(1-x)\frac{|\Phi(\zeta)|^2}{\zeta^4}, \tag{46}$$

where $\zeta^2 = x(1-x)\mathbf{b}_\perp^2$. Here $\mathbf{b}_\perp$ is the impact separation and Fourier conjugate to $\mathbf{k}_\perp$.

B. Holographic light-front representation

The mapping of the holographic variable z from AdS space to the impact variable ζ in the LF frame allows the equations of motion in AdS space to be recast in the form of a light-front Hamiltonian equation [58]

$$H_{\rm LF}|\phi\rangle = \mathcal{M}^2|\phi\rangle, \tag{47}$$

a remarkable result which allows the discussion of the

AdS/CFT solutions in terms of light-front equations in physical $3+1$ space-time. To make more transparent the holographic connection between AdS_5 and the conformal quantum field theory defined at its asymptotic $z \to 0$ boundary, it is convenient to write the AdS metric (1) in terms of light-front coordinates $x^{\pm} = x^0 \pm x^3$ and $\mathbf{x}_\perp$

$$ds^2 = \frac{R^2}{z^2}(dx^+ dx^- - d\mathbf{x}_\perp^2 - dz^2). \tag{48}$$

To simplify the discussion we consider the propagation of massive scalar modes in AdS space described by the normalized solutions to the wave equation ($d = 4$)

$$[z^2\partial_z^2 - (d-1)z\partial_z + z^2\mathcal{M}^2 - (\mu R)^2]\Phi(z) = 0, \tag{49}$$

where μ is the five-dimensional mass. Since the field Φ couples to a local boundary interpolating operator of dimension Δ, $\mathcal{O}_\Delta$, μ is determined by the relation $(\mu R)^2 = \Delta(\Delta - 4)$ between the fifth-dimensional mass of Φ and its scaling dimension. For spin-carrying constituents, the dimension of the operator is replaced by its twist τ, dimension minus spin, $\tau = \Delta - \sigma$, $\sigma = \sum_{i=1}^n \sigma_i$. For example $\tau = 2$ for a meson.

By substituting

$$\phi(\zeta) = \left(\frac{\zeta}{R}\right)^{-3/2}\Phi(\zeta), \tag{50}$$

in (49) we find an effective Schrödinger equation as a function of the weighted impact variable ζ

$$\left[-\frac{d^2}{d\zeta^2} + V(\zeta)\right]\phi(\zeta) = \mathcal{M}^2\phi(\zeta), \tag{51}$$

with $-\frac{d^2}{d\zeta^2}$ the light-front kinetic energy operator and

$$V(\zeta) = -\frac{1-4L^2}{4\zeta^2}, \tag{52}$$

the effective potential in the conformal limit, where we identify ζ with the fifth dimension z of AdS space: $\zeta = z$. We have written above $(\mu R)^2 = -4 + L^2$, for the fifth-dimensional mass μ appearing in the AdS wave equation. The effective wave Eq. (51) is a relativistic light-front equation defined at $x^+ = 0$. The AdS metric ds^2 (48) is invariant if $\mathbf{x}_\perp^2 \to \lambda^2\mathbf{x}_\perp^2$ and $z \to \lambda z$ at equal light-front time. The Casimir operator for the rotation group $SO(2)$ in the transverse light-front plane is L^2. This shows the natural holographic connection to the light front.

The Breitenlohner-Freedman stability bound [74]

$$(\mu R)^2 \geq -\frac{d^2}{4}, \tag{53}$$

requires $L^2 \geq 0$, thus the lowest state corresponds to $L = 0$. Higher excitations are matched to the small z asymptotic behavior of each string mode to the corresponding conformal dimension of the boundary operators of each hadronic state. In the semiclassical approximation the solution for mesons with relative orbital angular momentum L corresponds to an effective five-dimensional mass on the bulk side. The allowed values of μR are determined by requiring that asymptotically the dimensions become spaced by integers. The solution to (51) is

$$\phi(\zeta) = \zeta^{-3/2}\Phi(\zeta) = C\zeta^{1/2}J_L(\zeta\mathcal{M}). \tag{54}$$

The holographic light-front wavefunction $\phi(\zeta) = \langle\zeta|\phi\rangle$ is normalized according to

$$\langle\phi|\phi\rangle = \int d\zeta|\langle\zeta|\phi\rangle|^2 = 1, \tag{55}$$

and represents the probability amplitude to find n partons at transverse impact separation $\zeta = z$. Furthermore, its eigenmodes determine the hadronic mass spectrum [39]. For the truncated-space model the eigenvalues are determined by the boundary conditions at $\phi(z = 1/\Lambda_{\rm QCD}) = 0$ and are given in terms of the roots of Bessel functions: $\mathcal{M}_{L,k} = \beta_{L,k}\Lambda_{\rm QCD}$. [75]

A closed form of the light-front wavefunctions $\tilde{\psi}(x, \mathbf{b}_\perp)$ in the hard-wall model follows from (46)

$$\tilde{\psi}_{L,k}(x, \mathbf{b}_\perp) = \frac{\Lambda_{\rm QCD}}{\sqrt{\pi}J_{1+L}(\beta_{L,k})}\sqrt{x(1-x)} \times J_L(\sqrt{x(1-x)}|\mathbf{b}_\perp|\beta_{L,k}\Lambda_{\rm QCD}) \times \theta\left(\mathbf{b}_\perp^2 \leq \frac{\Lambda_{\rm QCD}^{-2}}{x(1-x)}\right). \tag{56}$$

The resulting wavefunction depicted in Fig. 1 displays confinement at large interquark separation and conformal symmetry at short distances, reproducing dimensional counting rules for hard exclusive amplitudes and the conformal properties of the LFWFs at high relative momenta in agreement with perturbative QCD.

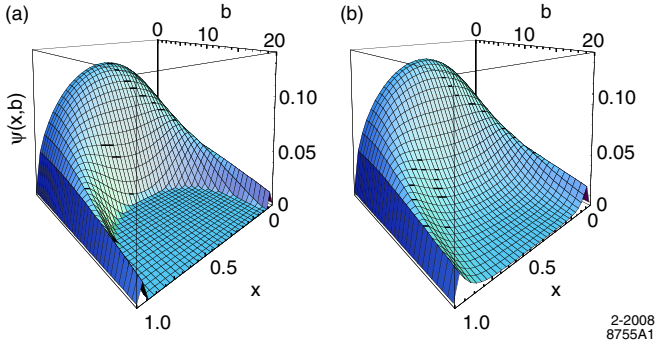

FIG. 1 (color online). AdS/QCD Predictions for the ground state light-front wavefunction of a pion in impact space. (a) Truncated-space model for $\Lambda_{\rm QCD} = 0.22$ GeV. (b) Soft-wall model for $\kappa = 0.375$ GeV.

VI. SOFT-WALL HOLOGRAPHIC MODEL

The predicted mass spectrum in the truncated-space hard-wall (HW) model is linear $M \propto L$ at high orbital

angular momentum L, in contrast to the quadratic dependence $M^2 \propto L$ in the usual Regge parametrization. It has been shown recently that by choosing a specific profile for a nonconstant dilaton, the usual Regge dependence can be obtained [10]. The procedure allows one to retain conformal AdS metrics (1) and to introduce a smooth cutoff which depends on the profile of a dilaton background field φ

$$S = \int d^4x dz \sqrt{g} e^{-\varphi(z)} \mathcal{L}, \tag{57}$$

where φ is a function of the holographic coordinate z which vanishes in the ultraviolet limit $z \to 0$. The IR hard-wall or truncated-space holographic model, discussed in the previous section, corresponds to a constant dilaton field $\varphi(z) = \varphi_0$ in the confining region, $z \leq 1/\Lambda_{\rm QCD}$, and to very large values elsewhere: $\varphi(z) \to \infty$ for $z > 1/\Lambda_{\rm QCD}$. The introduction of a soft cutoff avoids the ambiguities in the choice of boundary conditions at the infrared wall. A convenient choice [10] for the background field with usual Regge behavior is $\varphi(z) = \kappa^2 z^2$. The resulting wave equations are equivalent to the radial equation of a two-dimensional oscillator, previously found in the context of mode propagation on $\mathrm{AdS}_5 \times S^5$, in the light-cone formulation of Type II supergravity [76]. Also, equivalent results follow from the introduction of a Gaussian warp factor in the AdS metric for the particular case of massless vector modes propagating in the distorted metric [77].

A. Light-front mapping in the soft-wall model

We consider the propagation in AdS space of an electromagnetic probe polarized along Minkowski coordinates. Since the non-normalizable modes also couple to the dilaton field we must study the solutions of the modified wave equation

$$[z^2 \partial_z^2 - z(1 + 2\kappa^2 z^2)\partial_z - Q^2 z^2] J_\kappa(Q^2, z) = 0, \tag{58}$$

subject to the boundary conditions (35). The solution is

$$J_\kappa(Q^2, z) = \Gamma\left(1 + \frac{Q^2}{4\kappa^2}\right) U\left(\frac{Q^2}{4\kappa^2}, 0, \kappa^2 z^2\right), \tag{59}$$

where $U(a, b, c)$ is the confluent hypergeometric function.

The form factor in AdS space in presence of the dilaton background $\varphi = \kappa^2 z^2$ has the additional term $e^{-\kappa^2 z^2}$ in the metric

$$F(Q^2) = R^3 \int \frac{dz}{z^3} e^{-\kappa^2 z^2} \Phi(z) J_\kappa(Q^2, z) \Phi(z), \tag{60}$$

to be normalized to the charge operator at $Q = 0$. In the large Q^2 limit, $Q^2 \gg 4\kappa^2$, we find (Appendix C)

$$J_\kappa(Q^2, z) \to z Q K_1(zQ) = J(Q^2, z). \tag{61}$$

Thus, for large transverse momentum the current decouples from the dilaton field, and we recover our previous scaling results for the ultraviolet behavior of matrix elements.

To obtain the corresponding basis set of LFWFs we compare the DYW expression of the form factor (41) with the AdS form factor (60) for large values of Q, where (61) is valid. Thus, in the large Q limit we can identify the light-front spectator density with the corresponding AdS density

$$\tilde{\rho}(x, \zeta) = \frac{R^3}{2\pi} \frac{x}{1 - x} e^{-\kappa^2 \zeta^2} \frac{|\Phi(\zeta)|^2}{\zeta^4}. \tag{62}$$

When summed over all Fock states, the Drell-Yan-West formula gives an exact result. The formula describes the coupling of the free electromagnetic current to the elementary constituents in the interaction representation. In the presence of a dilaton field in AdS space, or in the case where the electromagnetic probe propagates in modified confining AdS metrics, the electromagnetic AdS mode is no longer dual to the free quark current, but dual to a dressed current, i.e., a hadronic electromagnetic current including virtual $\bar{q}q$ pairs and thus confined. Consequently, at finite values of the momentum transfer Q^2 our simple identification discussed above has to be reinterpreted since we are comparing states in different representations: the interaction representation in light-cone QCD versus the Heisenberg representation in AdS. However both quantities should represent the same observables. We thus expect that the modified mapping corresponds to the presence of higher Fock states in the hadron.

B. Holographic light-front representation

The equations of motion for scalar modes with smooth boundary conditions can also be recast in the form of a light-cone Hamiltonian form $H_{\rm LC}|\phi\rangle = \mathcal{M}^2|\phi\rangle$, with effective potential

$$V(\zeta) = -\frac{1 - 4L^2}{4\zeta^2} + \kappa^4 \zeta^2 + 2\kappa^2 (L - 1), \tag{63}$$

in the covariant light-front effective Schrödinger Equation (51). The effective potential describes transverse oscillations in the light-front plane with $SO(2)$ rotation subgroup and Casimir invariant L^2, representing LF rotations for the transverse coordinates. The solution to Eq. (51) for the potential (63) is

$$\phi(\zeta) = \kappa^{1+L} \sqrt{\frac{2n!}{(n + L)!}} \zeta^{1/2+L} e^{-\kappa^2 \zeta^2/2} L_n^L(\kappa^2 \zeta^2), \tag{64}$$

with eigenvalues

$$\mathcal{M}^2 = 4\kappa^2 (n + L). \tag{65}$$

The lowest stable solution corresponds to $n = L = 0$. With this choice for the potential, the lowest possible state is a zero mode in the spectrum, which can be identified with the pion.

Upon the substitution

$$\Phi(\zeta) = e^{\kappa^2\zeta^2/2}\left(\frac{\zeta}{R}\right)^{3/2}\phi(\zeta), \qquad \zeta \to z, \tag{66}$$

we express the solution (64) as the scalar mode

$$\Phi(z) = \frac{\kappa^{1+L}}{R^{(3/2)}}\sqrt{\frac{2n!}{(n+L)!}}z^{2+L}L_n^L(\kappa^2 z^2) \tag{67}$$

of scaling dimension $\Delta = 2 + L$ propagating in AdS space. A closed form of the light-front wavefunctions $\tilde{\psi}(x, \mathbf{b}_\perp)$ for a two-parton state in the soft-wall model then follows from (62),

$$\tilde{\psi}(x, \mathbf{b}_\perp) = \frac{\kappa^{L+1}}{\sqrt{\pi}}\sqrt{\frac{n!}{(n+L)!}}[x(1-x)]^{(1/2)+L}|\mathbf{b}_\perp|^L \times e^{-(1/2)\kappa^2 x(1-x)\mathbf{b}_\perp^2}L_n^L(\kappa^2 x(1-x)\mathbf{b}_\perp^2). \tag{68}$$

The resulting wavefunction for the pion is compared in Fig. 1 with the hard-wall result.

VII. PION FORM FACTOR

We compute the pion form factor from the AdS expressions (39) and (60) for the hadronic string modes Φ_π in the HW

$$\Phi_\pi^{\mathrm{HW}}(z) = \frac{\sqrt{2}\Lambda_{\mathrm{QCD}}}{R^{3/2}J_1(\beta_{0,1})}z^2 J_0(z\beta_{0,1}\Lambda_{\mathrm{QCD}}) \tag{69}$$

and soft-wall (SW) model

$$\Phi_\pi^{\mathrm{SW}}(z) = \frac{\sqrt{2}\kappa}{R^{3/2}}z^2, \tag{70}$$

respectively. We have obtained numerical results for both models. It was found recently that in the case of the SW model the results for form factors can be expressed analytically [36]. Thus, we shall extend the analytical results given in [36] to string modes with arbitrary scaling dimension τ, integer or not, allowing us to study the effect of anomalous dimensions in the expression for the form factors. This is described in Appendix D.

Since the pion mode couples to a twist-two boundary interpolating operator which creates a two-component hadronic bound state, the form factor is given in the SW model by the simple monopole form (D11) corresponding to $n = 2$

$$F_\pi(Q^2) = \frac{4\kappa^2}{4\kappa^2 + Q^2}, \tag{71}$$

the well known vector dominance model with the leading ρ resonance.

The hadronic scale is evaluated by fitting the spacelike data for the form factor as shown in Fig. 2, where we plot the product $Q^2F_\pi(Q^2)$ for the soft- and hard-wall holographic models. Both models would seem to describe the

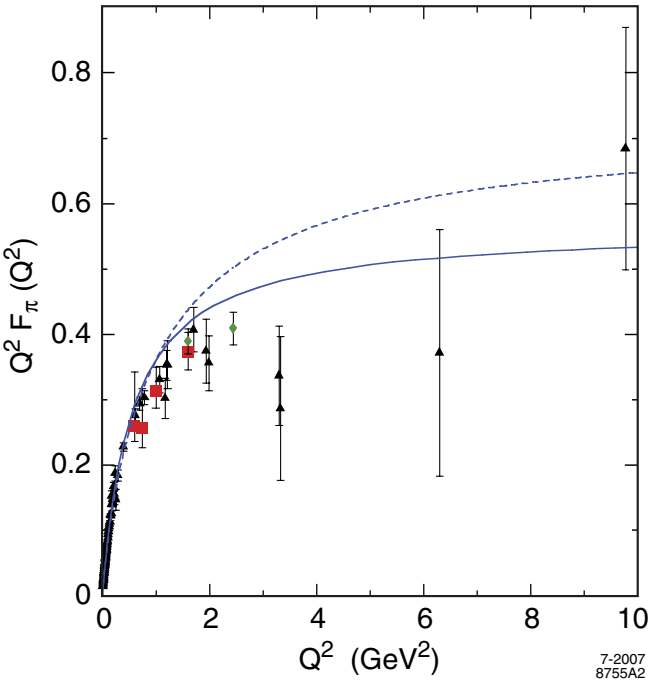

FIG. 2 (color online). Space-like scaling behavior for $Q^2F_\pi(Q^2)$ as a function of $Q^2 = -q^2$. The continuous line is the prediction of the soft-wall model for $\kappa = 0.375$ GeV. The dashed line is the prediction of the hard-wall model for $\Lambda_{\mathrm{QCD}} = 0.22$ GeV. The triangles are the data compilation from Baldini *et al.* [90], the boxes are JLAB 1 data [91] and diamonds are JLAB 2 data [92].

overall behavior of the spacelike data, with a better high-Q^2 description of scaling with the SW model. However, when the low energy data is examined in detail the SW model gives a noticeable better description as shown in Fig. 3. When the results for the pion form factor are analytically continued to the timelike region, $q^2 \to -q^2$ we obtain the results shown in Fig. 4 for $\log(|F_\pi(q^2)|)$. The monopole form of the SW model reproduces well the ρ peak with $M_\rho = 2\kappa = 750$ MeV and the scaling behavior in the spacelike region, but it does not give rise to the additional structure found in the timelike region, since the simple dipole form (71) is saturated by the ρ pole. The unconfined propagator $J(Q^2, z) = zQK_1(zQ)$ used in our description of the hard-wall model does not give rise to a pole structure in the timelike region, and thus fails to reproduce the ρ structure. When a small anomalous dimension is introduced, $\tau = 2 \pm \epsilon$, the formula (D9) for the form factor should be used instead. For a small deviation from the canonical value of two, the behavior in the spacelike region remains almost identical, but the form factor in the timelike region oscillates with infinite amplitude, and thus gives an unphysical solution.

In the strongly coupled semiclassical gauge/gravity limit hadrons have zero widths and are stable. One can nonetheless modify the formula (71) to introduce a finite width Γ

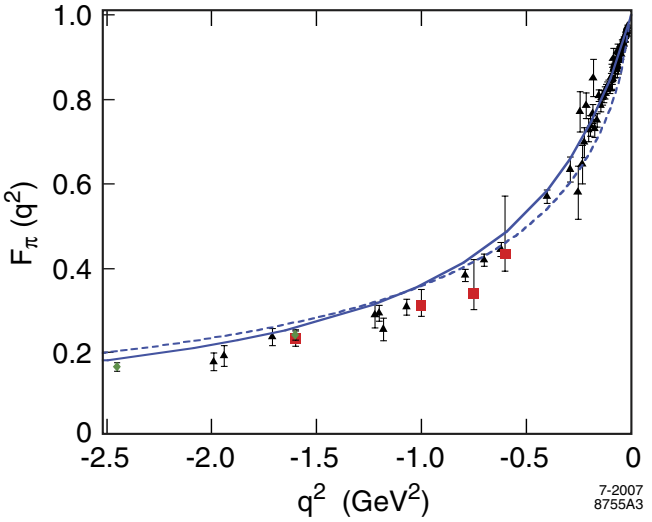

FIG. 3 (color online). Space-like behavior of the pion form factor $F_\pi(q^2)$ as a function of q^2 for $\kappa = 0.375$ GeV and $\Lambda_{\rm QCD} = 0.22$ GeV. Continuous line: soft-wall model, dashed line: hard-wall model. Triangles are the data compilation from Baldini *et al.* [90], boxes are JLAB 1 [91] and diamonds are JLAB 2 [92].

$$F_\pi(Q^2) = \frac{4\kappa^2}{4\kappa^2 - q^2 - 2i\kappa\Gamma}, \tag{72}$$

to compare with the pion form factor data near the ρ peak. The result is shown in Fig. 5. The corresponding phases for the pion form factor are shown in Fig. 6.

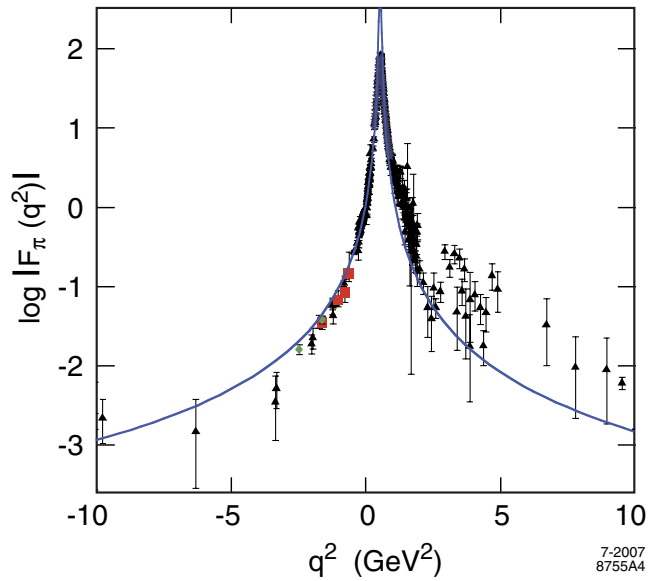

FIG. 4 (color online). Space and timelike behavior of the pion form factor $\log(|F_\pi(q^2)|)$ as a function of q^2 for $\kappa = 0.375$ GeV in the soft-wall model. Triangles are the data compilation from Baldini *et al.* [90], boxes are JLAB 1 [91] and diamonds are JLAB 2 [92].

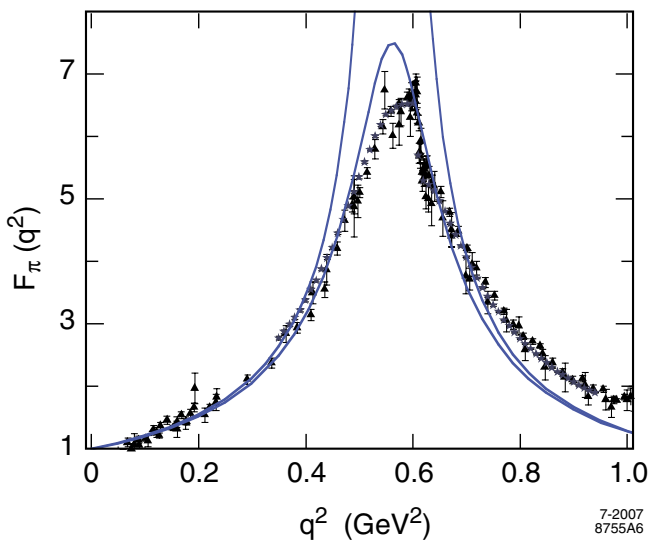

FIG. 5 (color online). Time-like pion form factor $|F_\pi(q^2)|$ near the ρ peak as a function of q^2 for $\kappa = 0.375$ GeV in the soft-wall model. The upper curve corresponds to $\Gamma = 0$ and the lower to $\Gamma = 100$ MeV. The data is from the compilation of Baldini *et al.* [90].

Using our results for the pion form factor one can extract the value of the mean pion charge radius squared through the small Q^2 expansion

$$F_\pi(Q^2) = 1 - \frac{1}{6}\langle r_\pi^2\rangle Q^2 + \mathcal{O}(Q^4), \tag{73}$$

and thus

$$\langle r_\pi^2\rangle = -6\frac{dF_\pi(Q^2)}{dQ^2}\bigg|_{Q^2=0}. \tag{74}$$

For the soft-wall model the form factor is given by the

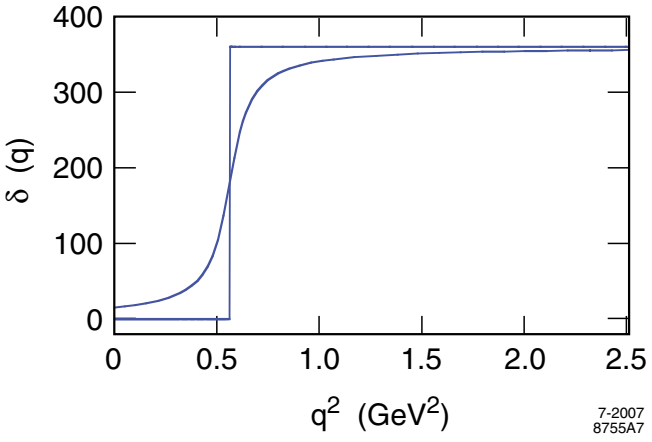

FIG. 6 (color online). Time-like pion form-factor phase $\delta_\pi(q)$ as a function of q^2 for $\kappa = 0.375$ GeV in the soft-wall model. The sharp curve corresponds to $\Gamma = 0$ and the smooth curve to $\Gamma = 100$ MeV.

monopole form (71) and we find

$$\langle r_\pi^2\rangle_{\rm SW} = \frac{3}{2\kappa^2} \simeq 0.42 \text{ fm}^2, \tag{75}$$

compared with the PDG value $\langle r_\pi^2\rangle = 0.45(1)$ fm^2 [78]. In the hard-wall model discussed in this paper the electromagnetic current is not confined and propagates in conformal metrics according to (36). To compute the second moment of the charge distribution $\langle r_\pi^2\rangle$ in this case, we expand $J(Q^2, z)$ in (37) for small values of Q^2

$$J(Q^2, z) = 1 + \frac{z^2Q^2}{4}\left[2\gamma - 1 + \ln\left(\frac{z^2Q^2}{4}\right)\right] + \mathcal{O}^4, \tag{76}$$

where γ, the Euler-Mascheroni constant, has the value $0.5772\ldots$ As there is no scale present in the expression for the bulk-to-boundary propagator (37), the value of $\langle r_\pi^2\rangle$ diverges logarithmically and thus the slope of the form factor is logarithmically divergent, although the predicted shape is consistent with the data except for very low Q^2. This formal problem in defining $\langle r_\pi^2\rangle$ does not appear if one uses Neumann boundary conditions for the HW model, and $\langle r_\pi^2\rangle \sim 1/\Lambda_{\rm QCD}^2$.

VIII. THE PION DECAY CONSTANT

The pion decay constant is given in terms of the matrix element of the axial isospin current $J^{\mu 5a}$ between a physical pion and the vacuum state [79]

$$\langle 0|J_a^{\mu 5}(x)|\pi_b(P)\rangle = -iP^\mu f_\pi \delta_{ab} e^{-iP\cdot x}. \tag{77}$$

The axial and vector currents are

$$J^{\mu 5a} = \bar{Q}\gamma^\mu\gamma^5 t^a Q, \qquad J^{\mu a} = \bar{Q}\gamma^\mu t^a Q \tag{78}$$

with Q the quark doublet

$$Q = \begin{pmatrix}\psi_u\\ \psi_d\end{pmatrix}, \tag{79}$$

and $t^a = \tau^a/2$ the generators of isospin rotations.

Consider the amplitude for the weak decay of a charged pion $\langle 0|J_W^+(0)|\pi^-(P^+, \vec{P}_\perp)\rangle$, where J_W^+ is the flavor changing weak current

$$J_W^+ = \bar{\psi}_u\gamma^+\frac{1}{2}(1-\gamma_5)\psi_d. \tag{80}$$

It follows that [80]

$$\langle 0|\bar{\psi}_u\gamma^+\frac{1}{2}(1-\gamma_5)\psi_d|\pi^-\rangle = i\frac{P^+ f_\pi}{\sqrt{2}}. \tag{81}$$

The expression for the current operator (80) in the particle number representation follows from the expansion of the field operator (13) in terms of quark creation and annihilation operators. The only terms which contribute to the annihilation process are the terms containing the product of operators d and b with opposite spin. Using the results listed in Appendix A for the quark spinor projections, we obtain the effective current operator

$$J_W^+ = \int \frac{dq^+ d^2\vec{q}_\perp}{(2\pi)^3}\int \frac{dq'^+ d^2\vec{q}'_\perp}{(2\pi)^3} d_{u\uparrow}(q) b_{d\downarrow}(q'), \tag{82}$$

in the limit of massless quarks. The flavor changing operator J_W^+ annihilates a d-quark with momentum q' and spin-down along the z direction and a u-antiquark momentum q and spin-up. Only the valence state

$$|d\bar{u}\rangle = \frac{1}{\sqrt{N_C}}\frac{1}{\sqrt{2}}\sum_{c=1}^{N_C}(b_{cd\downarrow}^\dagger d_{cu\uparrow}^\dagger - b_{cd\uparrow}^\dagger d_{cu\downarrow}^\dagger)|0\rangle, \tag{83}$$

with $L_z = 0$, $S_z = 0$, contributes to the decay of the $\pi^\pm$. Expanding the hadronic initial state in the amplitude (81) into its Fock components we find

$$f_\pi = 2\sqrt{N_C}\int_0^1 dx \int \frac{d^2\mathbf{k}_\perp}{16\pi^3}\psi_{\bar{q}q/\pi}(x, \mathbf{k}_\perp), \tag{84}$$

the light-cone equation which allows the exact computation of the pion decay constant in terms of the valence pion light-front wave function [48].

In terms of the distribution amplitude $\phi(x, Q)$

$$\phi(x, Q) = \int^{Q^2}\frac{d^2\mathbf{k}_\perp}{16\pi^3}\psi(x, \mathbf{k}_\perp), \tag{85}$$

it follows that

$$\phi_\pi(x, Q\to\infty) = \frac{4}{\sqrt{3}\pi} f_\pi\sqrt{x(1-x)}, \tag{86}$$

with

$$f_\pi = \frac{1}{8}\sqrt{\frac{3}{2}}R^{3/2}\lim_{\zeta\to 0}\frac{\Phi(\zeta)}{\zeta^2}, \tag{87}$$

since $\phi(x, Q\to\infty) \to \bar{\psi}(x, \mathbf{b}_\perp\to 0)/\sqrt{4\pi}$ as $\zeta\to 0$. The pion decay constant depends only on the behavior of the AdS string mode near the asymptotic boundary, $\zeta = z = 0$, and the mode normalization. For the hard-wall truncated-space pion mode (69) we find

$$f_\pi^{\rm HW} = \frac{\sqrt{3}}{8J_1(\beta_{0,k})}\Lambda_{\rm QCD} = 91.7 \text{ MeV}, \tag{88}$$

for $\Lambda_{\rm QCD} = 0.22$ MeV. The corresponding result for the soft-wall pion mode (70) is

$$f_\pi^{\rm SW} = \frac{\sqrt{3}}{8}\kappa = 81.2 \text{ MeV}, \tag{89}$$

for $\kappa = 0.375$ MeV. The values of $\Lambda_{\rm QCD}$ and κ are determined from the spacelike form-factor data as discussed above. The experimental result for f_π is extracted from the rate of weak π decay and has the value $f_\pi = 92.4$ MeV [78].

It is interesting to note that the pion distribution amplitude predicted by AdS/QCD (86) has a quite different x-behavior than the asymptotic distribution amplitude pre-

dicted from the perturbative quantum chromodynamics (PQCD) evolution [62] of the pion distribution amplitude $\phi_\pi(x, Q \to \infty) = \sqrt{3} f_\pi x(1-x)$. This observation appears to be consistent with the results of the Fermilab diffractive dijet experiment [81] which shows a broader x distribution for the dijets at small transverse momentum $k_\perp \leq 1$ GeV. The broader shape of the pion distribution increases the magnitude of the leading twist perturbative QCD prediction for the pion form factor by a factor of 16/9 compared to the prediction based on the asymptotic form, bringing the PQCD prediction close to the empirical pion form factor [37].

IX. CONCLUSIONS

One of the key difficulties in studies of quantum chromodynamics has been the absence of an analytic first approximation to the theory which not only can reproduce the hadronic spectrum, but also provides a good description of hadron wavefunctions. The AdS/CFT correspondence provides an elegant semiclassical approximation to QCD, which incorporates both color confinement and the conformal short-distance behavior appropriate for a theory with an infrared fixed point. Since the hadronic solutions are controlled by their twist dimension z^τ at small z, one also reproduces dimensional counting rules for hard exclusive processes. The AdS/CFT approach thus allows one to construct a model of hadrons which has both confinement at large distances and the conformal scaling properties which reproduce dimensional counting rules for hard exclusive reactions. The fundamental equations of AdS/CFT for mesons have the appearance of a radial Schrödinger Coulomb equation, but they are relativistic, covariant, and analytically tractable. The eigenvalues of the AdS/CFT equations provide a good description of the meson and baryon spectra for light quarks [8,11,39], and its eigensolutions provide a remarkably simple but realistic model of their valence wavefunctions. One can also derive analogous equations for baryons composed of massless quarks using a Dirac matrix representation for the baryon system [34].

The lowest stable state of the AdS equations is determined by the Breitenlohner-Freedman bound [74]. We can model confinement by imposing Dirichlet boundary conditions at $\phi(z = 1/\Lambda_{\rm QCD}) = 0$. The eigenvalues are then given in terms of the roots of the Bessel functions: $\mathcal{M}_{L,k} = \beta_{L,k}\Lambda_{\rm QCD}$. Alternatively, one can introduce a dilaton field [10] which provides a confinement potential $-\kappa^2\zeta^2$ to the effective potential $V(\zeta)$. The resulting hadron spectra are given by linear Regge trajectories in the square of the hadron masses, $\mathcal{M}^2$, characteristic of the Nambu string model. The AdS/CFT equations are integrable and thus the radial and orbital excitations can be obtained from ladder operators [34].

In this work we have shown that the eigensolutions $\Phi_H(z)$ of the AdS/CFT equations in the fifth dimension z have a remarkable mapping to the light-front wavefunctions $\psi_H(x_i, \mathbf{b}_{\perp i})$, the hadronic amplitudes which describe the valence constituents of hadrons in physical space-time, but at fixed light-cone time $\tau = t + z/c = 0$. Similarly, the AdS/CFT equations for hadrons can be mapped to equivalent light-front equations. The correspondence of AdS/CFT amplitudes to the QCD wavefunctions in light-front coordinates in physical space-time provides an exact holographic mapping at all energy scales between string modes in AdS space and hadronic boundary states. Most important, the eigensolutions of the AdS/CFT equation can be mapped to light-front equations of the hadrons in physical space-time, thus providing an elegant description of the light hadrons at the amplitude level.

The mapping of AdS/CFT string modes to light-front wave functions thus provides a remarkable analytic first approximation to QCD. Since they are complete and orthonormal, the AdS/CFT model wavefunctions can also be used as a basis for the diagonalization of the full light-front QCD Hamiltonian, thus systematically improving the AdS/CFT approximation.

We have also shown the correspondence between the expressions for current matrix elements in AdS/CFT with the corresponding expressions for form factors as given in the light-front formalism. In first approximation, where one takes the current propagating in a nonconfining background, one obtains the Drell-Yan West formula for valence Fock states, corresponding to the interaction picture of the light-front theory. Hadron form factors can thus be directly predicted from the overlap integrals in AdS space or equivalently by using the Drell-Yan-West formula in physical space-time. The form factor at high Q^2 receives its main contributions from small $\zeta \sim 1/Q$, corresponding to small $|\mathbf{b}_\perp| = \mathcal{O}(1/Q)$ and $1 - x = \mathcal{O}(1/Q)$. We have also shown how to improve this approximation by studying the propagation of non-normalizable solutions representing the electromagnetic current in a modified AdS confining metric, or equivalently in a dilaton background. This improvement in the description of the current corresponds in the light-front to multiple hadronic Fock states. The introduction of the confined current implies that the timelike form factors of hadrons will be mediated by vector mesons, including radial excitations. The wavefunction of the normalizable vector meson states $\mathcal{A}(z)$ appearing in the spectral decomposition of the Green's function described in Appendix C, which is dual to the non-normalizable photon propagation mode in AdS, is twist-3. This is the expected result for even parity axial mesons in QCD, or $L = 1$ odd parity vector mesons composed of a scalar squark and antisquarks. In the case of quark-antiquark states, one also expects to find $C = -1$, twist-2 meson solutions for the zero helicity component of the ρ with $S = 1$ and $L = 0$, which is supposed to give a dominant contribution to the ρ form factor.

We have applied our formulation to both the spacelike and timelike pion form factor. The description of the pion

form factor in the spacelike domain is in good agreement with experiment in both confinement models, the hard- and the soft-wall holographic models, but the hard-wall model discussed here fails to reproduce the very low Q^2 data. In particular, the mean pion charge radius squared $\langle r_\pi^2 \rangle$ diverges logarithmically. In the soft-wall model the timelike pion form factor exhibits a pole at the ρ mass with zero width since hadrons are stable in this theory, but it does not reproduce the additional resonant structure found in the timelike region. If one allows a width, the height of the ρ pole is in reasonable agreement with experiment. The spacelike Dirac form factor for the proton is also very well reproduced by the double-pole analytic expression shown in Appendix D for the case $N = 3$. This will be discussed elsewhere.

The deeply virtual Compton amplitude in the handbag approximation can be expressed as overlap of light-front wavefunctions [61]. The deeply virtual Compton amplitudes can be Fourier transformed to $b_\perp$ and $\sigma = x^- P^+/2$ space providing new insights into QCD distributions [82–86]. The distributions in the light-front direction σ typically display diffraction patterns arising from the interference of the initial and final state LFWFs [85,87]. All of these processes can provide detailed tests of the AdS/CFT LFWFs predictions.

The phenomenology of the AdS/CFT model is just beginning, but it can be anticipated that it will have many applications to QCD phenomena at the amplitude level. For example, the model LFWFs obtained from AdS/QCD provide a basis for understanding hadron structure functions and fragmentation functions at the amplitude level; the same wavefunctions can describe hadron formation from the coalescence of comoving quarks. The spin correlations which underlie single and double spin correlations are also described by the AdS/CFT eigensolutions. The AdS/CFT hadronic wavefunctions also provide predictions for the generalized parton distributions of hadrons and their weak decay amplitudes from first principles. The amplitudes relevant to diffractive reactions could also be computed. We also anticipate that the extension of the AdS/CFT formalism to heavy quarks will allow a great variety of heavy hadron phenomena to be analyzed from first principles.

ACKNOWLEDGMENTS

This research was supported by the Department of Energy Contract No. DE-AC02-76SF00515. The research of G. d. T. is supported in part by an Aportes grant from Florida Ice and Farm. We thank Oleg Andreev, Garth Huber, Cheng-Ryong Ji, Leonid Glozman, Bernard Pire, Anatoly Radyushkin, Giovanni Salmè and James Vary for helpful comments.

After finishing this paper, two new papers discussing the pion form factor including chiral symmetry breaking effects using the framework introduced in [9,16] in AdS/CFT, were posted into the arXiv. See [93,94]. In the approach of [9,16] the axial and vector currents become the primary entities as in effective chiral theory, in contrast with the framework described here where all mesons are quark-antiquark composites.

APPENDIX A: LIGHT-CONE SPINORS

In the light-cone (LC) formalism, spinors are written as [48]

$$u^\uparrow(p) = \frac{1}{\sqrt{p^+}}(p^+ + \beta m + \vec{\alpha}_\perp \cdot \mathbf{p}_\perp)\chi^\uparrow, \tag{A1}$$

$$v^\uparrow(p) = \frac{1}{\sqrt{p^+}}(p^+ - \beta m + \vec{\alpha}_\perp \cdot \mathbf{p}_\perp)\chi^\downarrow, \tag{A2}$$

with representation matrices

$$\vec{\alpha} = \begin{pmatrix} 0 & \vec{\sigma} \\ \vec{\sigma} & 0 \end{pmatrix}, \qquad \beta = \begin{pmatrix} I & 0 \\ 0 & -I \end{pmatrix}, \qquad \gamma_5 = \begin{pmatrix} 0 & I \\ I & 0 \end{pmatrix}, \tag{A3}$$

and spinors

$$\chi^\uparrow = \frac{1}{\sqrt{2}}\begin{pmatrix} 1 \\ 0 \\ 1 \\ 0 \end{pmatrix}, \qquad \chi^\downarrow = \frac{1}{\sqrt{2}}\begin{pmatrix} 0 \\ 1 \\ 0 \\ -1 \end{pmatrix}. \tag{A4}$$

The corresponding solutions for LC spinors $u^\downarrow(p)$ and $v^\downarrow(p)$ follow from reversing the spin component. Useful Dirac matrix elements for the helicity spinors are [48]

$$\bar{u}^\uparrow(\ell)\gamma^+ u^\uparrow(k) = \bar{u}^\downarrow(\ell)\gamma^+ u^\downarrow(k) = 2\sqrt{\ell^+ k^+}, \tag{A5}$$

$$\bar{u}^\downarrow(\ell)\gamma^+ u^\uparrow(k) = \bar{u}^\uparrow(\ell)\gamma^+ u^\downarrow(k) = 0, \tag{A6}$$

with $\bar{v}_\alpha(\ell)\gamma^\mu v_\beta(k) = \bar{u}_\beta(k)\gamma^\mu u_\alpha(\ell)$ and

$$\bar{v}^\downarrow(\ell)\gamma^+ u^\uparrow(k) = \bar{v}^\uparrow(\ell)\gamma^+ u^\downarrow(k) = 2\sqrt{\ell^+ k^+}, \tag{A7}$$

$$\bar{v}^\uparrow(\ell)\gamma^+ u^\uparrow(k) = \bar{v}^\downarrow(\ell)\gamma^+ u^\downarrow(k) = 0. \tag{A8}$$

It is simple to verify that

$$\frac{1}{2}(1 - \gamma_5)\chi^\uparrow = 0, \qquad \frac{1}{2}(1 - \gamma_5)\chi^\downarrow = \chi^\downarrow. \tag{A9}$$

Thus the chiral projection of the boosted LC spinors $u(p)$ and $v(p)$ in the limit of massless quarks

$$\frac{1}{2}(1 - \gamma_5)u^\downarrow(p) = u^\downarrow(p), \qquad \frac{1}{2}(1 - \gamma_5)u^\uparrow(p) = 0, \tag{A10}$$

$$\frac{1}{2}(1 - \gamma_5)v^\downarrow(p) = 0, \qquad \frac{1}{2}(1 - \gamma_5)v^\uparrow(p) = v^\uparrow(p), \tag{A11}$$

which follows from the fact that γ_5 commutes with $\vec{\alpha}_\perp$, but not with β. Consequently, in the massless limit we find that LC quark spinors with positive spin projection along the z-component also transform as right-handed spinors and LC spinors with negative spin projection are left-handed spinors. Also spinors representing massless antiquarks with positive spin component along the z-direction are left-handed and right-handed if polarized along the negative z-direction.

APPENDIX B: A USEFUL INTEGRAL

Consider the integral

$$J(Q^2, z) = \int_0^1 dx J_0\Big(zQ\sqrt{\frac{1-x}{x}}\Big). \tag{B1}$$

Changing the variable x according to $x = \frac{Q^2}{t^2+Q^2}$, we recast (B1) as

$$J(Q^2, z) = 2Q^2 \int_0^\infty \frac{tJ_0(zt)}{(t^2+Q^2)^2} dt, \tag{B2}$$

which is a Hankel-Nicholson type integral [88],

$$\int_0^\infty \frac{t^{\nu+1}J_\nu(zt)}{(t^2+a^2)^{\mu+1}} dt = \frac{z^\mu a^{\nu-\mu}}{2^\mu \Gamma(\mu+1)} K_{\nu-\mu}(az). \tag{B3}$$

Thus

$$J(Q^2, z) = QzK_1(zQ). \tag{B4}$$

APPENDIX C: BULK-TO-BOUNDARY PROPAGATOR IN THE SOFT-WALL MODEL

The bulk-to-boundary propagator in the soft-wall holographic model follows from the solution of the wave equation

$$[z^2\partial_z^2 - (1+2\kappa^2z^2)z\partial_z - Q^2z^2]J_\kappa(Q^2, z) = 0, \tag{C1}$$

describing the propagation of an electromagnetic probe in AdS space coupled to a dilaton background field $\varphi(z) = \kappa^2z^2$. The solution to (C1) subject to the boundary conditions

$$J_\kappa(Q^2 = 0, z) = J_\kappa(Q^2, z = 0) = 1, \tag{C2}$$

is

$$J_\kappa(Q^2, z) = \Gamma\Big(1 + \frac{Q^2}{4\kappa^2}\Big) U\Big(\frac{Q^2}{4\kappa^2}, 0, \kappa^2z^2\Big). \tag{C3}$$

Using the integral representation of the confluent hypergeometric function $U(a, b, z)$ [89]

$$\Gamma(a)U(a, b, z) = \int_0^\infty e^{-zt}t^{a-1}(1+t)^{b-a-1}dt, \tag{C4}$$

we find

$$J_\kappa(Q^2, z) = \frac{Q^2}{4\kappa^2} \int_0^\infty e^{-\kappa^2z^2t}\Big(\frac{1+t}{t}\Big)^{-(Q^2/4\kappa^2)} \frac{dt}{t(1+t)}. \tag{C5}$$

Making the change of variable $t = \frac{Q^2}{4\kappa^2}\mu$ and taking the limit $Q^2 \gg \kappa^2$

$$J_\kappa(Q^2 \to \infty, z) = \int_0^\infty \frac{d\mu}{\mu^2} \exp\Big(-\frac{z^2Q^2}{4}\mu - \frac{1}{\mu}\Big). \tag{C6}$$

Comparing the above expression with the integral representation of the modified Bessel function $K_\nu(z)$

$$K_\nu(z) = \frac{1}{2}\Big(\frac{z}{2}\Big)^\nu \int_0^\infty \frac{e^{-t-(z^2/4t)}}{t^{\nu+1}} dt, \tag{C7}$$

we find

$$\lim_{Q^2\to\infty} J_\kappa(Q^2, z) = zQK_1(zQ). \tag{C8}$$

In the large Q^2 limit the electromagnetic probe in AdS space decouples from the dilaton background.

1. Green's function formalism

In a finite spatial dimension the Green's function has a spectral decomposition in terms of eigenfunctions. Normalizable spin-one modes propagating on AdS_5 have polarization and plane waves along Minkowski coordinates $\mathcal{A}(x, z)_\mu = e^{-iP\cdot x}\mathcal{A}(z)\epsilon_\mu$, with invariant mass $P_\mu P^\mu = \mathcal{M}^2$. The eigenfunctions are determined by the eigenvalue equation

$$[-z^2\partial_z^2 + (1+2\kappa^2z^2)z\partial_z]\mathcal{A}_n(z) = M_n^2z^2\mathcal{A}_n(z), \tag{C9}$$

with solutions

$$\mathcal{A}_n(z) = \frac{\kappa^2}{R^{1/2}}\sqrt{\frac{2}{n+1}} z^2L_n^1(\kappa^2z^2), \tag{C10}$$

and eigenvalues

$$\mathcal{M}_n^2 = 4\kappa^2(n+1). \tag{C11}$$

The eigenfunctions $\mathcal{A}_n$ are orthonormal

$$R\int \frac{dz}{z} e^{-\kappa^2z^2}\mathcal{A}_n(z)\mathcal{A}_m(z) = \delta_{nm}, \tag{C12}$$

and satisfy the completeness relation

$$R\sum_n \frac{e^{-\kappa^2z'^2}}{z'} A_n(z')A_n(z) = \delta(z-z'). \tag{C13}$$

The Green's function is a solution of the homogeneous equation

$$[-z^2\partial_z^2 + (1+2\kappa^2z^2)z\partial_z - q^2z^2]G(z, z'; q) = -\delta(z-z'), \tag{C14}$$

where $q^2 = -Q^2 \le 0$. Since the eigenfunctions $\mathcal{A}_n$ form

a complete basis we can perform a spectral expansion of the Green's function

$$G(z, z'; q) = R\sum_{nm} a_{nm}(Q)\frac{e^{-\kappa^2 z'^2}}{z'}\mathcal{A}_n(z')\mathcal{A}_m(z). \quad \text{(C15)}$$

Substituting the above expression in (C14) and using (C13) the expansion coefficients a_{nm} are determined. We find

$$G(z, z'; q) = \sum_n \frac{\mathcal{A}_n(z')\mathcal{A}_n(z)}{q^2 - M_n^2 + i\epsilon}. \quad \text{(C16)}$$

2. Relation with the results of Grigoryan and Radyushkin

Performing the change of variable $t = \frac{x}{1-x}$ in the integral representation for the bulk-to-boundary propagator (C5), and integrating by parts the resulting expression, there follows

$$J_\kappa(Q^2, z) = \kappa^2 z^2 \int_0^1 \frac{dx}{(1-x)^2} x^{(Q^2/4\kappa^2)} e^{-\kappa^2 z^2 x/(1-x)}, \quad \text{(C17)}$$

the result found by Grigoryan and Radyuskin in [36]. It was also pointed out in [36] that the integrand in (C17) contains the generating function of the associated Laguerre polynomials

$$\frac{e^{-\kappa^2 z^2 x/(1-x)}}{(1-x)^{k+1}} = \sum_{n=0}^{\infty} L_n^k(\kappa^2 z^2) x^n, \quad \text{(C18)}$$

and thus $J_\kappa(Q^2, z)$ can be expressed as a sum of poles [36]

$$J_\kappa(Q^2, z) = 4\kappa^4 z^2 \sum_{n=0}^{\infty} \frac{L_n^1(\kappa^2 z^2)}{Q^2 + M_n^2}, \quad \text{(C19)}$$

with M_n^2 given by (C11). The above result also follows immediately from (C16) using the expression

$$J(Q^2, z) = J(Q^2, 0)\lim_{z'\to 0}\frac{R}{z'} e^{-\kappa^2 z'^2}\partial_{z'} G(z, z'; q), \quad \text{(C20)}$$

which defines the bulk-to-boundary propagator in terms of the Green's function [38].

APPENDIX D: ANALYTIC SOLUTION OF STRUCTURE FUNCTIONS AND FORM FACTORS FOR ARBITRARY TWIST IN THE SOFT-WALL MODEL

A string mode Φ_τ in the soft-wall model representing the lowest radial $n = 0$ node

$$\Phi_\tau(z) = \frac{1}{R^{3/2}}\sqrt{\frac{2}{\Gamma(\tau-1)}}\kappa^{\tau-1} z^\tau \quad \text{(D1)}$$

is normalized according to

$$\langle\Phi_\tau|\Phi_\tau\rangle = R^3\int\frac{dz}{z^3} e^{-\kappa^2 z^2}\Phi_\tau(z)^2 = 1. \quad \text{(D2)}$$

Since the field Φ_τ couples to a local hadronic interpolating operator of twist τ defined at the asymptotic boundary of AdS space, the scaling dimension of Φ_τ is τ.

1. The structure function

To compute the structure function $q(x)$

$$\int_0^1 dx q(x) = 1, \quad \text{(D3)}$$

corresponding to the string mode Φ_τ, we substitute the integral representation of the unit operator in the warped geometry of the soft-wall model

$$\mathbf{1} = \kappa^2 z^2 \int_0^1 \frac{dx}{(1-x)^2} e^{-\kappa^2 z^2 x/(1-x)}, \quad \text{(D4)}$$

in the normalization condition (D2): $\langle\Phi_\tau|\mathbf{1}|\Phi_\tau\rangle$. Upon integration over the coordinate z we find

$$q(x) = (\tau-1)(1-x)^{\tau-2}, \quad \text{(D5)}$$

which gives a constant x-dependence for a two-parton hadronic bound state. Equation (D4) follows from (C17) in the limit $Q = 0$.

2. Hadronic form factor

Likewise, we can compute the hadronic form factor in the soft-wall holographic model

$$F(Q^2) = R^3\int\frac{dz}{z^3} e^{-\kappa^2 z^2}\Phi_\tau(z) J_\kappa(Q^2, z)\Phi_\tau(z), \quad \text{(D6)}$$

by substituting the integral representation (C17) for $J_\kappa(q, z)$ in (D6) and integrating over the variable z. We find the result

$$F(Q^2) = \int_0^1 dx\rho(x, Q), \quad \text{(D7)}$$

where

$$\rho(x, Q) = (\tau-1)(1-x)^{\tau-2} x^{(Q^2/4\kappa^2)}. \quad \text{(D8)}$$

The integral (D7) can be expressed in terms of gamma functions. The final result for the form factor is

$$F(Q^2) = \Gamma(\tau)\frac{\Gamma(1+\frac{Q^2}{4\kappa^2})}{\Gamma(\tau+\frac{Q^2}{4\kappa^2})}. \quad \text{(D9)}$$

In the absence of anomalous dimensions the twist is an integer, $\tau = N$, and we can simplify (D9) by using the recurrence formula

$$\Gamma(N+z) = (N-1+z)(N-2+z)\ldots(1+z)\Gamma(1+z). \quad \text{(D10)}$$

We find

$$F(Q^2) = \frac{1}{1+\frac{Q^2}{4\kappa^2}}, \qquad N = 2, \tag{D11}$$

$$F(Q^2) = \frac{2}{(1+\frac{Q^2}{4\kappa^2})(2+\frac{Q^2}{4\kappa^2})}, \qquad N = 3, \tag{D12}$$

$$\cdots$$

$$F(Q^2) = \frac{(N-1)!}{(1+\frac{Q^2}{4\kappa^2})(2+\frac{Q^2}{4\kappa^2})\cdots(N-1+\frac{Q^2}{4\kappa^2})}, \qquad N, \tag{D13}$$

which is expressed as an $N-1$ product of poles, corresponding to the first $N-1$ states along the vector meson radial trajectory. For large Q^2 it follows that

$$F(Q^2) \to (N-1)!\left[\frac{4\kappa^2}{Q^2}\right]^{(N-1)}, \tag{D14}$$

and we recover the power law counting rules for hard scattering.

APPENDIX E: CONTRIBUTIONS TO MESON FORM FACTORS AND STRUCTURE FUNCTIONS AT LARGE MOMENTUM TRANSFER IN ADS/QCD

The form factor of a hadron at large Q^2 arises from the small z kinematic domain in AdS space. According to the AdS/CFT duality, this corresponds to small distances $x^\mu x_\mu \sim 1/Q^2$ in physical space-time, the domain where the current matrix elements are controlled by the conformal twist dimension, Δ, of the hadron's interpolating operator. In the case of the front form, where $x^+ = 0$, this corresponds to small transverse separation $x^\mu x_\mu = -\mathbf{x}_\perp^2$.

As we have shown in [39], one can use holography to map the functional form of the string modes $\Phi(z)$ in AdS space to the light-front wavefunctions in physical space-time by identifying z with the transverse variable $\zeta = \sqrt{\frac{x}{1-x}}|\vec{\eta}_\perp|$. Here $\vec{\eta}_\perp = \sum_{i=1}^{n-1} x_i \mathbf{b}_{\perp i}$ is the weighted impact separation, summed over the impact separation of the spectator constituents. The leading large-Q^2 behavior of form factors in AdS/QCD arises from small $\zeta \sim 1/Q$, corresponding to small transverse separation.

For the case of a meson with two constituents the form factor can be written in terms of an effective light-front transverse density in impact space. From (30)

$$F(q^2) = \int_0^1 dx \int db^2 \tilde{\rho}(x, b, Q), \tag{E1}$$

with $\tilde{\rho}(x, b, Q) = \pi J_0(bQ(1-x))|\tilde{\psi}(x, b)|^2$ and $b = |\mathbf{b}_\perp|$. The kinematics are illustrated in Fig. 7 for the case of a meson with two constituents in the soft-wall model

$$\tilde{\psi}_{q\bar{q}/\pi}(x, \mathbf{b}_\perp) = \frac{\kappa}{\sqrt{\pi}}\sqrt{x(1-x)}\, e^{-(1/2)\kappa^2 x(1-x)\mathbf{b}_\perp^2}, \tag{E2}$$

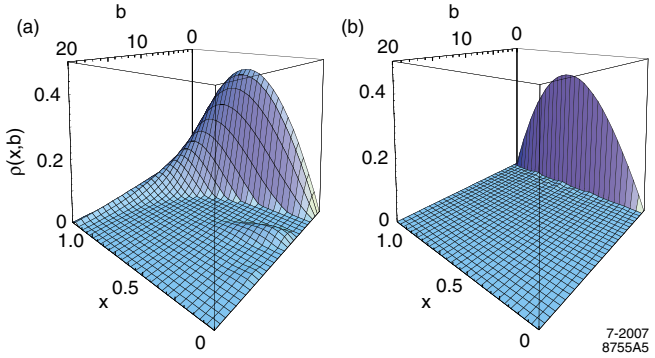

FIG. 7 (color online). Effective partonic density $\tilde{\rho}(x, b, Q)$ in terms of the longitudinal momentum fraction x, the transverse relative impact variable $b = |\mathbf{b}_\perp|$ and momentum transfer Q for the soft-wall model. As Q increases the distribution becomes increasingly important near $x = 1$ and $\mathbf{b}_\perp = 0$. This is illustrated in (a) for $Q = 1$ GeV/c. At very large Q (b), the distribution is peaked towards $\mathbf{b}_\perp = 0$. The value of κ is 0.375 GeV.

where the Gaussian form of the LFWF favors short-distance configurations with small $\zeta^2 = b_\perp^2 x(1-x) \sim 1/Q^2$. Since we are mainly interested in studying the contribution from different regions to the form factor at large Q^2, we have replaced the modified bulk-to-boundary propagator $J_\kappa(Q, z)$ (59) by its large Q^2 form $zQK_1(zQ)$. One sees a shift of the integrand $\tilde{\rho}(x, b, Q)$ toward small $|\mathbf{b}_\perp|$ and small $1-x$ at high Q^2. A similar behavior is observed for the LFWF obtained from the hard-wall model.

The physical situation in momentum space is somewhat more complicated. The LFWF in $\mathbf{k}_\perp$ space is the Fourier transform

$$\psi(x, k) = 4\pi^{3/2}\int_0^\infty b db J_0(kb)\tilde{\psi}(x, b), \tag{E3}$$

with $k = |\mathbf{k}_\perp|$. Thus

$$\psi_{\bar{q}q/\pi}(x, \mathbf{k}_\perp) = \frac{4\pi}{\kappa\sqrt{x(1-x)}}\, e^{-(\mathbf{k}_\perp^2/2\kappa^2 x(1-x))}, \tag{E4}$$

with exponential falloff at high relative transverse momentum. The Drell-Yan-West light-front expression (26) for the form factor for a two-parton bound state has the form

$$F(q^2) = \int_0^1 dx \int \frac{d^2\mathbf{k}_\perp}{16\pi^3}\sum_q e_q \psi^*_{P'}(x, \mathbf{k}_\perp + (1-x)\mathbf{q}_\perp) \times \psi_P(x, \mathbf{k}_\perp). \tag{E5}$$

The form factor can be written in terms of a density in x, $\mathbf{k}_\perp$ space:

$$F(Q^2) = \int_0^1 dx \int dk^2 \rho(x, k, Q), \tag{E6}$$

where

$$\rho(x,k,Q)=\frac{1}{\kappa^2}\frac{1}{x(1-x)}I_0\left(\frac{kQ}{\kappa^2 x}\right)e^{-((1-x)Q^2/2\kappa^2 x)}\times e^{-(\mathbf{k}_\perp^2/\kappa^2 x(1-x))}. \tag{E7}$$

In this case the large Q^2 behavior comes from the regime $1-x\sim\kappa^2/Q^2$ and $k_\perp^2\sim x(1-x)\kappa^2\sim\kappa^4/Q^2$. Note that the $x\to 1$ domain for finite $k_\perp$ (or nonzero quark mass) implies $x_j=k_j^+/P^+\to 0$ for each spectator, a regime of high relative longitudinal momentum since the limit $k^+\to 0$ requires $k^z\simeq -k^0$; i.e., $k_z^2\gg\mathbf{k}_\perp^2$ for each spectator.

Integration over k in Eq. (E6) gives

$$F(Q^2)=\int_0^1 dx e^{-((1-x)Q^2/4\kappa^2 x)}, \tag{E8}$$

which is identical to the result obtained in the transverse impact representation after integration over $\mathbf{b}_\perp$. The above expression for the form factor in the soft-wall model is valid for relatively high Q^2 since we have approximated the bulk-to-boundary propagator by its asymptotic form. In the limit $Q^2\gg\kappa^2$ we find

$$F_\pi(Q^2)\to\frac{4\kappa^2}{Q^2}, \tag{E9}$$

the scaling result for a two-constituent meson at large Q^2 found in Appendix D.

The pion structure function $q_\pi(x,Q^2)$ is computed by integrating the square of the pion LFWF (E4) up to the scale Q^2

$$q_\pi(x,Q^2)=\int^{Q^2}\frac{d^2\mathbf{k}_\perp}{16\pi^3}|\psi_{\bar{q}q/\pi}(x,\mathbf{k}_\perp)|^2. \tag{E10}$$

We find

$$q_\pi(x,Q^2)=1-e^{-(Q^2/\kappa^2 x(1-x))}. \tag{E11}$$

In the large Q^2 limit $q_\pi(x,Q^2\to\infty)\equiv q_\pi(x)=1$, which is the behavior of a strongly coupled theory found in QCD(1 + 1) [59]. The result coincides with (D5) for $\tau=2$. Identical results [32] are obtained for the pion in the hard-wall model, $q(x)=1$.

[1] J. M. Maldacena, Adv. Theor. Math. Phys. **2**, 231 (1998) [Int. J. Theor. Phys. **38**, 1113 (1999)]; S. S. Gubser, I. R. Klebanov, and A. M. Polyakov, Phys. Lett. B **428**, 105 (1998); E. Witten, Adv. Theor. Math. Phys. **2**, 253 (1998).
[2] J. Polchinski and M. J. Strassler, Phys. Rev. Lett. **88**, 031601 (2002).
[3] R. A. Janik and R. Peschanski, Nucl. Phys. **B565**, 193 (2000).
[4] S. J. Brodsky and G. F. de Teramond, Phys. Lett. B **582**, 211 (2004).
[5] R. C. Brower, M. J. Strassler, and C. I. Tan, arXiv:0707.2408 and references therein.
[6] H. Boschi-Filho and N. R. F. Braga, J. High Energy Phys. 05 (2003) 009.
[7] G. F. de Teramond and S. J. Brodsky, arXiv:hep-th/0409074.
[8] G. F. de Teramond and S. J. Brodsky, Phys. Rev. Lett. **94**, 201601 (2005).
[9] J. Erlich, E. Katz, D. T. Son, and M. A. Stephanov, Phys. Rev. Lett. **95**, 261602 (2005).
[10] A. Karch, E. Katz, D. T. Son, and M. A. Stephanov, Phys. Rev. D **74**, 015005 (2006).
[11] G. F. de Teramond, arXiv:hep-ph/0606143.
[12] N. Evans and A. Tedder, Phys. Lett. B **642**, 546 (2006).
[13] D. K. Hong, T. Inami, and H. U. Yee, Phys. Lett. B **646**, 165 (2007).
[14] P. Colangelo, F. De Fazio, F. Jugeau, and S. Nicotri, Phys. Lett. B **652**, 73 (2007).
[15] H. Forkel, M. Beyer, and T. Frederico, J. High Energy Phys. 07 (2007) 077.
[16] L. Da Rold and A. Pomarol, Nucl. Phys. **B721**, 79 (2005); J. High Energy Phys. 01 (2006) 157.
[17] J. Hirn and V. Sanz, J. High Energy Phys. 12 (2005) 030; J. Hirn, N. Rius, and V. Sanz, Phys. Rev. D **73**, 085005 (2006).
[18] K. Ghoroku, N. Maru, M. Tachibana, and M. Yahiro, Phys. Lett. B **633**, 602 (2006).
[19] H. Boschi-Filho, N. R. F. Braga, and C. N. Ferreira, Phys. Rev. D **73**, 106006 (2006).
[20] O. Andreev and V. I. Zakharov, Phys. Rev. D **74**, 025023 (2006).
[21] T. Hambye, B. Hassanain, J. March-Russell, and M. Schvellinger, Phys. Rev. D **74**, 026003 (2006); Phys. Rev. D **76**, 125017 (2007).
[22] C. Csaki and M. Reece, J. High Energy Phys. 05 (2007) 062.
[23] J. Polchinski and M. J. Strassler, J. High Energy Phys. 05 (2003) 012.
[24] R. C. Brower, J. Polchinski, M. J. Strassler, and C. I. Tan, J. High Energy Phys. 12 (2007) 005.
[25] L. F. Alday and J. Maldacena, J. High Energy Phys. 06 (2007) 064.
[26] J. Babington, J. Erdmenger, N. J. Evans, Z. Guralnik, and I. Kirsch, Phys. Rev. D **69**, 066007 (2004).
[27] I. Kirsch, J. High Energy Phys. 09 (2006) 052.
[28] R. Apreda, J. Erdmenger, D. Lust, and C. Sieg, J. High Energy Phys. 01 (2007) 079.
[29] K. Nawa, H. Suganuma, and T. Kojo, Phys. Rev. D **75**, 086003 (2007).
[30] D. K. Hong, M. Rho, H. U. Yee, and P. Yi, Phys. Rev. D **76**,

061901 (2007); J. High Energy Phys. 09 (2007) 063.
[31] H. Hata, T. Sakai, S. Sugimoto, and S. Yamato, arXiv:hep-th/0701280.
[32] A. V. Radyushkin, Phys. Lett. B **642**, 459 (2006).
[33] S. J. Brodsky, arXiv:hep-ph/0608005.
[34] S. J. Brodsky and G. F. de Teramond, arXiv:hep-th/0702205.
[35] H. R. Grigoryan and A. V. Radyushkin, Phys. Lett. B **650**, 421 (2007).
[36] H. R. Grigoryan and A. V. Radyushkin, Phys. Rev. D **76**, 095007 (2007).
[37] For a different but complementary approach see for example H. M. Choi and C. R. Ji, Phys. Rev. D **74**, 093010 (2006). See also, T. Gousset and B. Pire, Phys. Rev. D **51**, 15 (1995); J. P. B. de Melo, T. Frederico, E. Pace, and G. Salme, Phys. Rev. D **73**, 074013 (2006) and references therein.
[38] S. Hong, S. Yoon, and M. J. Strassler, J. High Energy Phys. 04 (2006) 003; arXiv:hep-ph/0501197.
[39] S. J. Brodsky and G. F. de Teramond, Phys. Rev. Lett. **96**, 201601 (2006).
[40] L. von Smekal, R. Alkofer, and A. Hauck, Phys. Rev. Lett. **79**, 3591 (1997).
[41] D. Zwanziger, Phys. Rev. D **69**, 016002 (2004).
[42] R. Alkofer, C. S. Fischer, and F. J. Llanes-Estrada, Phys. Lett. B **611**, 279 (2005).
[43] D. Epple, H. Reinhardt, and W. Schleifenbaum, Phys. Rev. D **75**, 045011 (2007).
[44] A. Deur, V. Burkert, J. P. Chen, and W. Korsch, Phys. Lett. B **650**, 244 (2007).
[45] S. J. Brodsky, S. Menke, C. Merino, and J. Rathsman, Phys. Rev. D **67**, 055008 (2003).
[46] S. J. Brodsky, J. R. Pelaez, and N. Toumbas, Phys. Rev. D **60**, 037501 (1999).
[47] S. Furui and H. Nakajima, Phys. Rev. D **76**, 054509 (2007); Braz. J. Phys. **37**, 186 (2007).
[48] G. P. Lepage and S. J. Brodsky, Phys. Rev. D **22**, 2157 (1980).
[49] M. Diehl, T. Feldmann, R. Jakob, and P. Kroll, Eur. Phys. J. C **39**, 1 (2005).
[50] S. J. Brodsky and H. J. Lu, Phys. Rev. D **51**, 3652 (1995).
[51] S. J. Brodsky, G. T. Gabadadze, A. L. Kataev, and H. J. Lu, Phys. Lett. B **372**, 133 (1996).
[52] S. J. Brodsky, G. P. Lepage, and P. B. Mackenzie, Phys. Rev. D **28**, 228 (1983).
[53] S. J. Brodsky, M. S. Gill, M. Melles, and J. Rathsman, Phys. Rev. D **58**, 116006 (1998).
[54] M. Binger and S. J. Brodsky, Phys. Rev. D **74**, 054016 (2006).
[55] J. M. Cornwall and J. Papavassiliou, Phys. Rev. D **40**, 3474 (1989).
[56] M. Binger and S. J. Brodsky, Phys. Rev. D **69**, 095007 (2004).
[57] P. A. M. Dirac, Rev. Mod. Phys. **21**, 392 (1949).
[58] S. J. Brodsky, H. C. Pauli, and S. S. Pinsky, Phys. Rep. **301**, 299 (1998).
[59] H. C. Pauli and S. J. Brodsky, Phys. Rev. D **32**, 2001 (1985); K. Hornbostel, S. J. Brodsky, and H. C. Pauli, Phys. Rev. D **41**, 3814 (1990).
[60] S. J. Brodsky and D. S. Hwang, Nucl. Phys. **B543**, 239 (1999).
[61] S. J. Brodsky, M. Diehl, and D. S. Hwang, Nucl. Phys. **B596**, 99 (2001).
[62] G. P. Lepage and S. J. Brodsky, Phys. Lett. **87B**, 359 (1979).
[63] A. V. Efremov and A. V. Radyushkin, Phys. Lett. **94B**, 245 (1980).
[64] S. J. Brodsky and G. P. Lepage, Report No. SLAC-PUB-2294, 1979.
[65] S. J. Brodsky, D. S. Hwang, B. Q. Ma, and I. Schmidt, Nucl. Phys. **B593**, 311 (2001).
[66] S. D. Drell and T. M. Yan, Phys. Rev. Lett. **24**, 181 (1970).
[67] G. B. West, Phys. Rev. Lett. **24**, 1206 (1970).
[68] D. E. Soper, Phys. Rev. D **15**, 1141 (1977).
[69] In the study of generalized parton distributions (GPDs) the transverse distance between the active quark and the center of mass momentum, $\vec{\eta}_\perp = \sum_{j=1}^{n-1} x_j \mathbf{b}_{\perp j}$, is often referred to as $\mathbf{b}_\perp$, whereas the internal transverse coordinates, labeled here $\mathbf{b}_{\perp i}$, conjugate to the relative transverse momentum coordinates $\mathbf{k}_{\perp i}$, are labeled $\mathbf{c}_{\perp i}$. See M. Burkardt and D. S. Hwang, Phys. Rev. D **69**, 074032 (2004).
[70] S. J. Brodsky and S. D. Drell, Phys. Rev. D **22**, 2236 (1980).
[71] J. Polchinski and L. Susskind, arXiv:hep-th/0112204.
[72] S. J. Brodsky and G. R. Farrar, Phys. Rev. Lett. **31**, 1153 (1973); G. P. Lepage and S. J. Brodsky, Phys. Rev. D **22**, 2157 (1980).
[73] V. A. Matveev, R. M. Muradian, and A. N. Tavkhelidze, Lett. Nuovo Cimento Soc. Ital. Fis. **7**, 719 (1973).
[74] P. Breitenlohner and D. Z. Freedman, Ann. Phys. (N.Y.) **144**, 249 (1982).
[75] It is not possible to obtain physically reasonable light-front wave functions satisfying Neumann boundary conditions at the infrared boundary, $\partial_n \phi(z)|_{z=z_0} = 0$, since hadronic LFWFs are expected to vanish at the confinement radius $1/\Lambda_{\rm QCD}$ [35].
[76] R. R. Metsaev, arXiv:hep-th/0002008.
[77] O. Andreev, Phys. Rev. D **73**, 107901 (2006).
[78] S. Eidelman *et al.* (Particle Data Group), Phys. Lett. B **592**, 1 (2004).
[79] M. E. Peskin and D. V. Schroeder, *An Introduction to Quantum Field Theory* (Addison-Wesley Publishing Company, Reading, MA, 1995).
[80] In obtaining (81) we have used the isospin charge eigenstate basis $|\pi^\pm\rangle = \frac{1}{\sqrt{2}}(|\pi^1\rangle \pm i|\pi^2\rangle)$, and the relation [79] $\bar{u}\gamma^\mu(1-\gamma^5)d = j^{\mu 1} + ij^{\mu 2} - j^{\mu 51} - ij^{\mu 52}$.
[81] E. M. Aitala *et al.* (E791 Collaboration), Phys. Rev. Lett. **86**, 4768 (2001).
[82] M. Burkardt, Int. J. Mod. Phys. A **21**, 926 (2006).
[83] X. d. Ji, Phys. Rev. Lett. **91**, 062001 (2003).
[84] J. P. Ralston and B. Pire, Phys. Rev. D **66**, 111501 (2002).
[85] S. J. Brodsky, D. Chakrabarti, A. Harindranath, A. Mukherjee, and J. P. Vary, Phys. Lett. B **641**, 440 (2006).
[86] P. Hoyer, AIP Conf. Proc. **904**, 65 (2007).
[87] S. J. Brodsky, D. Chakrabarti, A. Harindranath, A. Mukherjee, and J. P. Vary, Phys. Rev. D **75**, 014003 (2007).
[88] M. Abramowitz and I. Stegun, *Handbook of Mathematical Functions* (Dover, New York, 1970), p. 488.
[89] M. Abramowitz and I. Stegun, *Handbook of Mathematical*

Functions (Dover, New York, 1970), p. 505.
[90] R. Baldini, S. Dubnicka, P. Gauzzi, S. Pacetti, E. Pasqualucci, and Y. Srivastava, Eur. Phys. J. C **11**, 709 (1999).
[91] V. Tadevosyan *et al.* (Jefferson Lab F(pi) Collaboration), Phys. Rev. C **75**, 055205 (2007).
[92] T. Horn *et al.* (Fpi2 Collaboration), Phys. Rev. Lett. **97**, 192001 (2006).
[93] H. J. Kwee and R. F. Lebed, arXiv:0708.4054.
[94] H. R. Grigoryan and A. V. Radyushkin, arXiv:0709.0500.